

Pursuit of a Discriminative Representation for Multiple Subspaces via Sequential Games

Druv Pai, Michael Psenka, Chih-Yuan Chiu, Manxi Wu, Edgar Dobriban, Yi Ma*

June 22, 2022

Abstract

We consider the problem of learning discriminative representations for data in a high-dimensional space with distribution supported on or around multiple low-dimensional linear subspaces. That is, we wish to compute a linear injective map of the data such that the features lie on multiple *orthogonal* subspaces. Instead of treating this learning problem using multiple PCAs, we cast it as a sequential game using the closed-loop transcription (CTRL) framework recently proposed for learning discriminative and generative representations for general low-dimensional submanifolds. We prove that the equilibrium solutions to the game indeed give correct representations. Our approach unifies classical methods of learning subspaces with modern deep learning practice, by showing that subspace learning problems may be provably solved using the modern toolkit of representation learning. In addition, our work provides the first theoretical justification for the CTRL framework, in the important case of linear subspaces. We support our theoretical findings with compelling empirical evidence. We also generalize the sequential game formulation to more general representation learning problems. Our code, including methods for easy reproduction of experimental results, is [publicly available on GitHub](#).

1 Motivation and Context

Learning representations of complex high-dimensional data with low underlying complexity is a central goal in machine learning, with applications to compression, sampling, out-of-distribution detection, classification, etc. For example, in the context of image data, one may perform clustering [40], and generate or detect fake images [23]. There are a number of recently popular methods for representation learning, several proposed in the context of image generation; one such example is generative adversarial networks (GANs) [18], giving promising results [27, 37]. Despite empirical successes, theoretical understanding of representation learning of high-dimensional data with low complexity is still in its infancy. Classical methods with theoretical guarantees, such as principal component analysis (PCA) [25], are divorced from modern methods such as GANs whose justifications are mostly empirical and whose theoretical properties remain poorly understood [13, 15].

A challenge for our theoretical understanding is that *high-dimensional data often has low-dimensional structure*, such as belonging to multiple subspaces and even nonlinear manifolds [14, 33, 34, 41, 42, 50, 52, 53, 54]. This hypothesis can be difficult to account for theoretically.¹ In fact, our understanding of this setting, and knowledge of principled and generalizable solutions, is still incomplete, even in the case when the data lies on multiple linear subspaces [49], and the representation map is linear.

In this work, we aim to bridge this gap. More specifically, we propose a new theoretically principled formulation, based on sequential game theory and modern representation learning, for learning discriminative

*D. Pai (druvpai@berkeley.edu), M. Psenka (psenka@berkeley.edu), C.Y. Chiu (chihyuan_chiu@berkeley.edu), and Y. Ma (yima@eecs.berkeley.edu) are with the Department of Electrical Engineering and Computer Sciences at the University of California, Berkeley. M. Wu (manxiwu@cornell.edu) is with the School of Operations Research and Information Engineering at Cornell University, and the Simons Institute for Theory of Computing at the University of California, Berkeley. E. Dobriban (dobriban@upenn.edu) is with the Department of Statistics and Data Science at the University of Pennsylvania.

¹One assumption which violates this hypothesis implicitly is the existence of a probability density for the data. For instance, the analysis in several prominent works on representation learning, such as [15, 29] critically requires this assumption to hold. Probability densities with respect to the Lebesgue measure on \mathbb{R}^n do not exist if the underlying probability measure has a Lebesgue measure zero support, e.g., for lower-dimensional structures such as subspaces [26]. Thus, this assumption excludes a lower dimensionality of the data.

representations with the multiple low-dimensional linear subspaces in high-dimensional space. We explicitly characterize the learned representations in this framework. Our results show that classical subspace learning problems can be solved using modern deep learning tools, thus unifying the classical and modern perspectives on this class of problems.

1.1 Related Works

PCA and Autoencoding. Principal component analysis (PCA) and its probabilistic versions [22, 45] are a classical tool for learning low-dimensional representations. One finds the best ℓ^2 -approximating subspace of a given dimension for the data. Thus, PCA can be viewed as *seeking to learn the linear subspace structure of the data*.

Several generalizations of PCA exist. Generalized PCA (GPCA) [48] *seeks to learn multiple linear subspace structure* by clustering. Unlike PCA and this work, GPCA does not learn transformed representations of the data. Here we learn discriminative representations of multiple linear subspace structure. PCA has also been adapted to recover nonlinear structures in many ways [47], e.g., via principal curves [19] or autoencoders [32].

GAN. Generative Adversarial Networks (GANs) are a recently popular representation learning method [1, 18]. GANs simultaneously learn a generator function, which maps low-dimensional noise to the data distribution, and a discriminator function, which maps the data to discriminative representations from which one can classify the data as authentic or synthetic with a simple predictor. The generator and discriminator are trained adversarially; the generator is trained to generate data which is distributionally close to real data, in order to fool the discriminator, while the discriminator is simultaneously trained to identify discrepancies between the generator output and empirical data.

While GANs enjoy empirical success (e.g. [27, 37]), their theoretical properties are less well developed, especially in the context of high-dimensional data with intrinsic structure. More specifically, the most prominent works of GAN analysis use the simplifying assumption of full-rank data [15], require explicit computation of objective functions which are intractable to even estimate using a finite sample [1, 55], or show how GANs have poor theoretical behavior, such as their training game not having Nash equilibria [13]. In this work, we adopt the more realistic assumption of low-dimensional data in a high-dimensional space, use explicit, closed-form objective functions which are more convenient to optimize (at least in the linear case), and demonstrate the existence of global equilibria of the training game corresponding to our method.

2 Preliminaries

2.1 Representation Learning

Suppose $\mathbf{X} \in \mathbb{R}^{d_x \times n}$ is a data matrix that contains $n \geq 1$ data points in \mathbb{R}^{d_x} . To model that the dimension of the support of \mathbf{x} is lower than the ambient dimension d_x , we consider data supported on *a union of k linear subspaces* $\bigcup_{j=1}^k \mathcal{S}_j \subseteq \mathbb{R}^{d_x}$, each of dimension $d_{\mathcal{S}_j} := \dim(\mathcal{S}_j)$. For each $j \in \{1, \dots, k\}$, let $\mathbf{X}_j \in \mathcal{S}_j^{n_j} \subseteq \mathbb{R}^{d_x \times n_j}$ be the matrix of the $n_j \geq 1$ columns of \mathbf{X} contained in \mathcal{S}_j , and let the *class information*, containing the assignment of each data point $\mathbf{x}^1, \dots, \mathbf{x}^n$ to its respective subspace index $j \in \{1, \dots, k\}$ be denoted by $\mathbf{\Pi}$.

The goal is to learn an encoder mapping $f: \mathbb{R}^{d_x} \rightarrow \mathbb{R}^{d_z}$, in some function class \mathcal{F} , such that $\mathbf{z} := f(\mathbf{x})$ takes values in \mathbb{R}^{d_z} . For representation learning, we want f to be such that $d_z \leq d_x$ and \mathbf{z} has better geometric properties, such as lying on orthogonal subspaces. Moreover, we want to learn an *inverse* or decoder mapping $g: \mathbb{R}^{d_z} \rightarrow \mathbb{R}^{d_x}$ in some function class \mathcal{G} , such that, for $\mathbf{x} \in D$, $(g \circ f)(\mathbf{x})$ is close to \mathbf{x} .

2.2 Closed-Loop Transcription

To learn the encoder mapping f and g , we use the Closed-Loop Transcription (CTRL) framework, a recent method proposed for representation learning of low-dimensional submanifolds in high-dimensional space [6]. This framework generalizes *both* GANs and autoencoders; as f has dual roles as an encoder and discriminator, and g has dual roles as a decoder and a generator.

For the data matrix \mathbf{X} , we define $f(\mathbf{X}) = [f(\mathbf{x}^1), \dots, f(\mathbf{x}^n)]$, and use similar notations throughout. The training process follows a *closed loop*: starting with the data \mathbf{X} and its representations $f(\mathbf{X})$, the

representations $(f \circ g \circ f)(\mathbf{X})$ of the autoencoded data $(g \circ f)(\mathbf{X})$ are used to train f and g . This approach has a crucial advantage over the GAN formulation: contrary to GANs [1, 55], since $f(\mathbf{X})$ and $(f \circ g \circ f)(\mathbf{X})$ both live in the structured representation space \mathbb{R}^{d_z} , interpretable measures of representation quality and of the difference between $f(\mathbf{X})$ and $(f \circ g \circ f)(\mathbf{X})$ exist and may be computed in *closed form*. These tractable measures are based on the paradigm of *rate reduction* [6, 51], which we briefly introduce here.

For $\varepsilon > 0$ and a matrix of representations $\mathbf{Z} \in \mathbb{R}^{d_z \times n}$, define

$$R(\mathbf{Z}) := \frac{1}{2} \log \det \left(\mathbf{I}_{d_z} + \frac{d_z}{n\varepsilon^2} \mathbf{Z} \mathbf{Z}^\top \right).$$

Suppose \mathbf{Z} is partitioned into $\mathbf{Z}_1, \dots, \mathbf{Z}_k$ by the class information $\mathbf{\Pi}$, where $\mathbf{Z}_j \in \mathbb{R}^{d_z \times n_j}$. Define

$$\Delta R(\mathbf{Z} \mid \mathbf{\Pi}) := R(\mathbf{Z}) - \sum_{j=1}^k \frac{n_j}{n} R(\mathbf{Z}_j).$$

Finally, for any two matrices $\mathbf{Z}_1, \mathbf{Z}_2 \in \mathbb{R}^{d_z \times n}$ of equal size, define (overloading notation slightly)

$$\Delta R(\mathbf{Z}_1, \mathbf{Z}_2) := R(\mathbf{Z}_1 \cup \mathbf{Z}_2) - \frac{1}{2} R(\mathbf{Z}_1) - \frac{1}{2} R(\mathbf{Z}_2).$$

The information-theoretic interpretations are as follows. We call $R(\mathbf{Z})$ the *coding rate* of \mathbf{Z} ; if the columns of \mathbf{Z} are sampled i.i.d. according to a zero-mean Gaussian vector, then $R(\mathbf{Z})$ is an estimate of the average number of bits required to encode the columns of \mathbf{Z} up to quantization error ε [5, 36]. Furthermore, $\Delta R(\mathbf{Z} \mid \mathbf{\Pi})$ is called the *rate reduction* of \mathbf{Z} with respect to $\mathbf{\Pi}$. If the columns of each \mathbf{Z}_j are sampled i.i.d. from a zero-mean multivariate Gaussian distribution, it approximates the average number of bits saved by encoding each representation matrix $\mathbf{Z}_1, \dots, \mathbf{Z}_k$ separately rather than all together as \mathbf{Z} . One should think of $\Delta R(\mathbf{Z} \mid \mathbf{\Pi})$ as a measure of expressiveness and discriminativeness of the representations [51]. Finally, $\Delta R(\mathbf{Z}_1, \mathbf{Z}_2)$ should be thought of as a measure of difference² between the two distributions generating the columns of \mathbf{Z}_1 and \mathbf{Z}_2 . For a more detailed discussion of rate reduction, see Appendix A.

2.3 Game Theoretic Formulation

Now that we have measures in the representation space for the properties we want to encourage in the encoder and decoder, we now discuss how to train the encoder function f and decoder function g .

Several methods, e.g., PCA [20], GAN [18], and the original CTRL formulation [6], can be viewed as learning the encoder (or discriminator) function f and decoder (or generator) function g via finding the Nash equilibria of an appropriate two-player *simultaneous* game between the encoder and decoder; we discuss this formulation further in Appendix B. In this work, we approach this problem from a different angle; we learn the encoder function f and decoder function g via an appropriate two-player *sequential* game between the encoder and the decoder; finding the so-called *Stackelberg equilibria*. We now cover the basics of sequential game theory; a more complete treatment is found in [2].

In a sequential game between the encoder — whose move corresponds to picking $f \in \mathcal{F}$ — and decoder — whose move corresponds to picking $g \in \mathcal{G}$ — both the encoder and the decoder attempt to maximize their own objectives, the so-called *utility functions* $u_{\text{enc}}: \mathcal{F} \times \mathcal{G} \rightarrow \mathbb{R}$ and $u_{\text{dec}}: \mathcal{F} \times \mathcal{G} \rightarrow \mathbb{R}$ respectively, by making their moves one at a time. In our formulation, the *encoder moves first*, and then the decoder aims to invert the encoder.

The solution concept for sequential games — that is, the encoder and decoder that correspond to rational actions — is the *Stackelberg equilibrium* [16, 24]. In our context, (f_\star, g_\star) is a Stackelberg equilibrium if and only if

$$f_\star \in \operatorname{argmax}_{f \in \mathcal{F}} \inf \left\{ u_{\text{enc}}(f, g) \mid g \in \operatorname{argmax}_{g \in \mathcal{G}} u_{\text{dec}}(f, g) \right\}, \quad g_\star \in \operatorname{argmax}_{g \in \mathcal{G}} u_{\text{dec}}(f_\star, g).$$

The sequential notion of the game is reflected in the definition of the equilibrium; the decoder, going second, may play g to maximize u_{dec} with full knowledge of the encoder’s play f , while the encoder plays f to maximize u_{enc} with only the knowledge that the decoder plays optimally.

²Note that $\Delta R(\cdot, \cdot)$ is not strictly a distance; for instance, $\Delta R(\mathbf{Z}_1, \mathbf{Z}_2) = 0$ does not imply that $\mathbf{Z}_1 = \mathbf{Z}_2$ or that the distributions generating \mathbf{Z}_1 and \mathbf{Z}_2 are the same.

While gradient descent-ascent (GDA) with equal learning rates for f and g does not suffice to learn Stackelberg equilibria in theory or in practice [24], GDA with lopsided learning rates [24] and GDMax [23, 24] converge to local notions of Stackelberg equilibria in theory. In practice, GDMax converges to Stackelberg equilibria in our examples. For more discussion on practical considerations, see Section 4.

3 Multiple-Subspace Pursuit via the CTRL Framework

With this background in place, we now introduce the closed-loop multi-subspace pursuit (CTRL-MSP) method. Recall that in Section 2.3 we discussed the idea of learning $f \in \mathcal{F}$ and $g \in \mathcal{G}$ as equilibria for a two-player sequential game. We now introduce the game in question.

Let $\mathcal{L}(\mathbb{R}^a, \mathbb{R}^b)$ be the set of linear maps from \mathbb{R}^a to \mathbb{R}^b . Let $\|\cdot\|_F : \mathbf{A} \mapsto \sqrt{\sum_{i,j} \mathbf{A}_{ij}^2}$ be the usual Frobenius norm on matrices.

Definition 1 (CTRL-MSP Game). *The CTRL-MSP game is a two-player sequential game between:*

1. *The encoder, moving first, choosing functions f in the function class*

$$\mathcal{F} := \{f \in \mathcal{L}(\mathbb{R}^{d_x}, \mathbb{R}^{d_z}) \mid \|f(\mathbf{X}_j)\|_F^2 \leq n_j, \forall j \in \{1, \dots, k\}\},$$

and having utility function

$$u_{\text{enc}}(f, g) := \Delta R(f(\mathbf{X}) \mid \mathbf{\Pi}) + \sum_{j=1}^k \Delta R(f(\mathbf{X}_j), (f \circ g \circ f)(\mathbf{X}_j)).$$

2. *The decoder, moving second, choosing functions g in the function class $\mathcal{G} := \mathcal{L}(\mathbb{R}^{d_z}, \mathbb{R}^{d_x})$, and having utility function*

$$u_{\text{dec}}(f, g) := - \sum_{j=1}^k \Delta R(f(\mathbf{X}_j), (f \circ g \circ f)(\mathbf{X}_j)).$$

Thus, the encoder f aims to maximize the discriminativeness $\Delta R(f(\mathbf{X}) \mid \mathbf{\Pi})$ of the representations $f(\mathbf{X})$, as well as the total difference $\sum_{j=1}^k \Delta R(f(\mathbf{X}_j), (f \circ g \circ f)(\mathbf{X}_j))$ between the representations $f(\mathbf{X}_j)$ and the closed-loop reconstructions $(f \circ g \circ f)(\mathbf{X}_j)$. The decoder g aims to minimize the latter. Since $\Delta R(f(\mathbf{X}) \mid \mathbf{\Pi})$ is not a function of g , this game may be alternatively posed as a *zero-sum* game. Keeping the same encoder utility, and setting $u_{\text{dec}}(f, g) = -u_{\text{enc}}(f, g)$, the learned equilibria would be the same. Zero-sum games enjoy rich convergence guarantees, albeit using more regularity than is present here [2, 7, 16], but we do not invoke the zero-sum structure further in this work.

Before we characterize the learned encoder and decoder in CTRL-MSP games, it is first worthwhile to discuss the qualitative properties we want them to have, and how we can achieve them quantitatively. Recall that we wish to learn an encoder-decoder pair $(f_*, g_*) \in \mathcal{F} \times \mathcal{G}$ such that the encoder is injective and discriminates between the data subspaces, and also is self-consistent. We study quantitative ways to measure these properties. As a notation, for two sets U, V , a map $h: U \rightarrow V$, and a subset $W \subseteq U$, we denote by $h(W) = \{h(u) \mid u \in W\}$ the image of W under h .

1. To enforce the *injectivity* of the encoder, we aim to ensure that each $f_*(\mathcal{S}_j)$ is a linear subspace of dimension equal to that of \mathcal{S}_j , and furthermore, we aim to enforce that $f_*(\mathbf{X}_j)$ should have no small nonzero singular values.
2. To discriminate between different subspaces, we aim to enforce the subspace representations $f_*(\mathcal{S}_j)$ to be orthogonal for different j .
3. To enforce internal *self-consistency*, we aim to have the subspace representations $f_*(\mathcal{S}_j)$ and the autoencoded subspace representations $(f_* \circ g_* \circ f_*)(\mathcal{S}_j)$ be equal.

We now explicitly characterize the Stackelberg equilibria in the CTRL-MSP game, and show how they connect to each of these properties. For a matrix $\mathbf{A} \in \mathbb{R}^{m \times n}$, let $\text{Col}(\mathbf{A}) \subseteq \mathbb{R}^n$ be the vector space spanned by the columns of \mathbf{A} . Let $\sigma_i(\mathbf{A})$, $1 \leq i \leq \min\{m, n\}$ be the singular values of \mathbf{A} sorted in non-increasing order. Finally, for subspaces S_1, S_2 , denote by $S_1 + S_2$ the sum vector space $\{\mathbf{s}_1 + \mathbf{s}_2 \mid \mathbf{s}_1 \in S_1, \mathbf{s}_2 \in S_2\}$. With these notations, our key assumptions are summarized below:

Assumption 2 (Assumptions in CTRL-MSP Games).

1. (Multiple classes) $k \geq 2$.
2. (Informative data) For each $j \in \{1, \dots, k\}$, $\text{Col}(\mathbf{X}_j) = S_j$.
3. (Large enough representation space.) $\sum_{j=1}^k d_{S_j} \leq \min\{d_x, d_z\}$.
4. (Incoherent class data) $\sum_{j=1}^k d_{S_j} = \dim(\sum_{j=1}^k S_j)$.³
5. (High coding precision) $\varepsilon^4 \leq \min_{j=1}^k (n_j/n \cdot d_z^2/d_{S_j}^2)$.

Our main result is:

Theorem 3 (Stackelberg Equilibria of CTRL-MSP Games). *If Assumption 2 holds, then the CTRL-MSP game has the following properties:*

1. A Stackelberg equilibrium (f_*, g_*) exists.
2. Any Stackelberg equilibrium (f_*, g_*) enjoys the following properties:
 - (a) (Injective encoder) For each $j \in \{1, \dots, k\}$, we have that $f_*(S_j)$ is a linear subspace of dimension d_{S_j} . Further, for each $j \in \{1, \dots, k\}$, one of the following holds:
 - $\sigma_1(f_*(\mathbf{X}_j)) = \dots = \sigma_{d_{S_j}}(f_*(\mathbf{X}_j)) = \frac{n_j}{d_{S_j}}$; or
 - $\sigma_1(f_*(\mathbf{X}_j)) = \dots = \sigma_{d_{S_j}-1}(f_*(\mathbf{X}_j)) \in (\frac{n_j}{d_{S_j}}, \frac{n_j}{d_{S_j}-1})$ and $\sigma_{d_{S_j}}(f_*(\mathbf{X}_j)) > 0$, where if $d_{S_j} = 1$ then $\frac{n}{d_{S_j}-1}$ is interpreted as $+\infty$.
 - (b) (Discriminative encoder) The subspaces $\{f_*(S_j)\}_{j=1}^k$ are orthogonal for distinct indices j .
 - (c) (Consistent encoding and decoding) For each $j \in \{1, \dots, k\}$, we have that $f_*(S_j) = (f_* \circ g_* \circ f_*)(S_j)$.

The proof of this theorem uses Theorem 6; proofs of both are left to Appendix C. Once in the framework of Theorem 6, the main difficulty is the characterization of the maximizers of $f \mapsto \Delta R(f(\mathbf{X}) \mid \mathbf{\Pi})$. This function is non-convex and challenging to analyze; we characterize it by carefully applying inequalities on the singular values of the representation matrices.

As the theorem indicates, the earlier check-list of desired quantitative properties can be achieved by CTRL-MSP. That is, CTRL-MSP provably learns injective and discriminative representations of multiple-subspace structure.

For the special case $k = 1$, where we are learning a single-subspace structure, it is possible to change the utility functions and function classes of CTRL-MSP, to learn a *different* set of properties that more closely mirrors PCA. In particular, a Stackelberg equilibrium encoder f_* of this modified game does not render the covariance of $f(\mathbf{X}_1)$ nearly-isotropic; it instead is an ℓ^2 -isometry on S_1 , which ensures well-behaved injectivity. The details are left to Appendix D.

We now discuss an implication of the CTRL-MSP method. The original problem statement of learning discriminative representations for multiple subspace structure may be solved directly via orthogonalizing the representations of multiple PCAs. However, CTRL-MSP provides an alternative approach: simultaneously learning and representing the subspaces via a modern representation learning toolkit. This gives a unifying perspective on classical and modern representation learning, by showing that classical methods can be viewed as *special cases* of modern methods, and that they may be formulated to learn the same types of representations. A major benefit (discussed further in Section 5) is that the new formulation can be readily generalized to much broader families of structures, beyond subspaces to submanifolds, as compelling empirical evidence in [6] demonstrates.

³An intuitive understanding of this condition is that if we take a linearly independent set from each S_j , the union of all these sets is still linearly independent.

4 Empirical Evaluation of CTRL-MSP

We demonstrate empirical convergence of CTRL-MSP to equilibria which satisfy the conclusions of Theorem 3, in both the benign case of nearly-orthogonal subspaces, and more correlated subspaces. We then demonstrate CTRL-MSP’s robustness to noise. For more details regarding the experimental setup, CTRL-MSP’s empirical properties, and experimental results clarifying the difference between CTRL-MSP and other popular representation learning algorithms, see Appendix E.

We fix baseline values of $n = 1500$, $k = 3$, $d_x = 50$, $d_z = 40$, $\varepsilon^2 = 1$, $d_{\mathcal{S}_1} = 3$, $d_{\mathcal{S}_2} = 4$, $d_{\mathcal{S}_3} = 5$, and $n_1 = n_2 = n_3 = n/k = 500$. Mini-batches of size $b = 50$ are randomly sampled during optimization. To generate data, we fix $\nu, \sigma^2 \geq 0$, and generate a single random matrix with orthonormal columns $\mathbf{Q} \in \mathbb{R}^{d_x \times (\max_j d_{\mathcal{S}_j})}$ using the QR decomposition. Then, for each subspace, we select $d_{\mathcal{S}_j}$ random columns from \mathbf{Q} uniformly without replacement to form a matrix $\mathbf{Q}_j \in \mathbb{R}^{d_x \times d_{\mathcal{S}_j}}$. We then generate random matrices $\Theta_j \in \mathbb{R}^{d_x \times d_x}$, $\xi_j \in \mathbb{R}^{d_{\mathcal{S}_j} \times n}$, $\tau_j \in \mathbb{R}^{d_x \times n}$ whose entries are i.i.d. standard normal random variables, and set $\tilde{\mathbf{Q}}_j$ to be the matrix whose columns are the normalized columns of $(\mathbf{I}_{d_x} + \nu \Theta_j) \mathbf{Q}_j$. We finally obtain $\mathbf{X}_j = \tilde{\mathbf{Q}}_j \xi_j + \sqrt{\frac{\sigma^2}{d_x}} \tau_j$. If ν is small, the generated data is highly coherent across subspaces; if ν is large, the data are incoherent, since high dimensional random vectors with near-independent entries are incoherent with high probability [50]. Thus, this data generation process allows us to test CTRL-MSP and other algorithms; on data with various correlation structures.

In each experiment, we measure the success of CTRL-MSP in three qualitative ways. Below, let $\|\cdot\|_{\ell^2}$ denote the standard ℓ^2 norm.

1. We check that that each column of $f_*(\mathbf{X}_j)$ is strongly correlated (or, coherent) with other columns in $f_*(\mathbf{X}_j)$, and nearly orthogonal to columns of $f_*(\mathbf{X}_\ell)$ for $\ell \neq j$. This may be checked via plotting the *heatmap* of pairwise absolute cosine similarities $(|\cos \angle(\mathbf{x}^p, \mathbf{x}^q)|)_{1 \leq p, q \leq n}$. We order our data points so that $\mathbf{X} = [\mathbf{X}_1 \ \mathbf{X}_2 \ \mathbf{X}_3]$, so we aim for this heatmap to be perfectly block diagonal.
2. We check that the spectra of each $f(\mathbf{X}_j)$ are as described by our theoretical results; there are $d_{\mathcal{S}_j}$ nonzero singular values, and they are close to each other.
3. We check that $f_*(\mathcal{S}_j) = (f_* \circ g_* \circ f_*)(\mathcal{S}_j)$. Since $f_*(\mathcal{S}_j) = \text{Col}(f_*(\mathbf{X}_j))$ and $(f_* \circ g_* \circ f_*)(\mathcal{S}_j) = \text{Col}((f_* \circ g_* \circ f_*)(\mathbf{X}_j))$, we test this by plotting the distribution of the projection residual given by $\left\| f_*(\mathbf{x}^i) - \text{proj}_{\text{Col}((f_* \circ g_* \circ f_*)(\mathbf{X}_j))} (f_*(\mathbf{x}^i)) \right\|_{\ell^2}$ for all \mathbf{x}^i which are columns of \mathbf{X}_j ; we aim for this value to be near-zero for most or all \mathbf{x}^i .

4.1 Benign Subspaces

In the first experiment, we set $\nu = 10^6$ and $\sigma^2 = 0$, which initializes the subspaces \mathcal{S}_j as incoherent. Figure 1 demonstrates the success of CTRL-MSP in this scenario: the cosine similarity heatmap presents a strong block diagonal, the representations corresponding to each subspace \mathcal{S}_j have $d_{\mathcal{S}_j}$ large singular values, and the subspaces are within a low projection distance of each other.

4.2 Highly Correlated Subspaces

In the second experiment, we set $\nu = 0.1$ and $\sigma^2 = 0$. This produces highly correlated subspaces. Yet, CTRL-MSP succeeds in this scenario: the cosine similarity heatmap presents a striking block diagonal structure, the representations corresponding to each subspace \mathcal{S}_j have $d_{\mathcal{S}_j}$ large non-zero singular values. Further, the subspaces have low projection distance to each other (Figure 2). We remark that this situation seems significantly more difficult than the previous scenario, yet the learned encoder and decoder achieve the same outcomes.

4.3 Highly Correlated and Noisy Subspaces

In the third experiment, we tackle the more difficult case of $\nu = 0.1$ and $\sigma^2 = 0.01$. This adds off-subspace noise to the data, which then no longer satisfies the assumptions of the theoretical analysis. However,

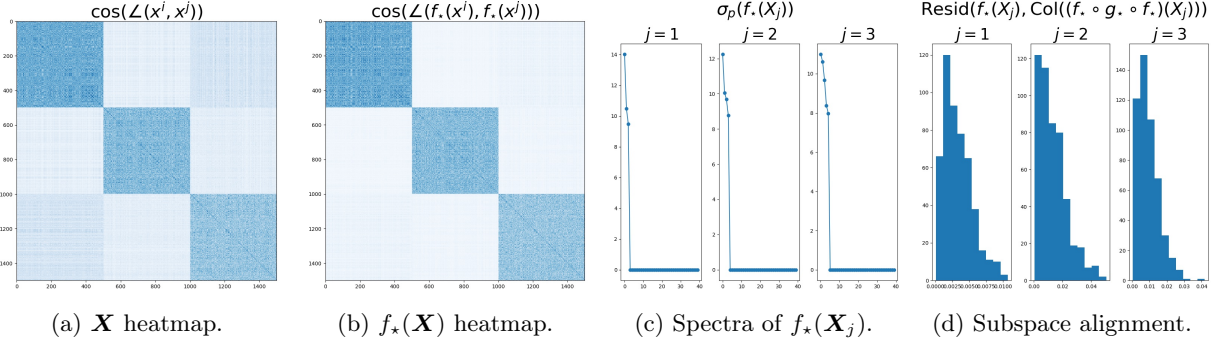


Figure 1: Behavior of CTRL-MSP on benign subspaces. (a) Original heatmap of correlations. (b) Heatmap of correlations of the learned representations. (c) Singular value spectra of the representation matrices of the three subspaces. (d) Histogram of norms of residuals $\left\| f_*(\mathbf{x}^i) - \text{proj}_{\text{Col}((f_* \circ g_* \circ f_*)(\mathbf{X}_j))}(f_*(\mathbf{x}^i)) \right\|_{\ell_2}$ for all \mathbf{x}^i which are columns of \mathbf{X}_j .

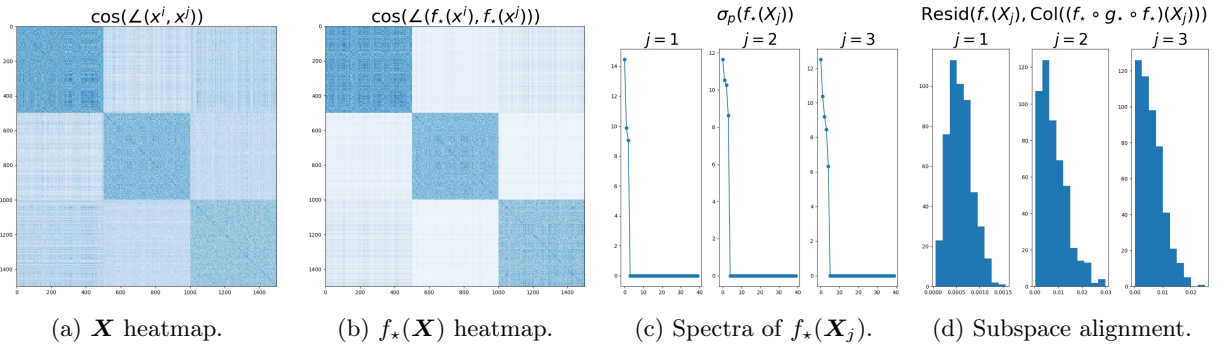


Figure 2: Behavior of CTRL-MSP on highly correlated subspaces, with the same plots as in Fig. 1.

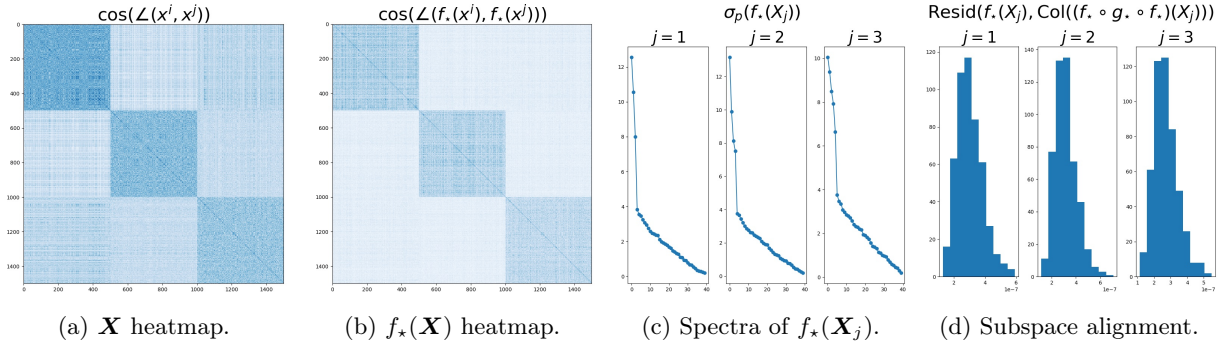


Figure 3: Behavior of CTRL-MSP on highly correlated and noisy subspaces. The same quantities as in Fig. 1 are plotted.

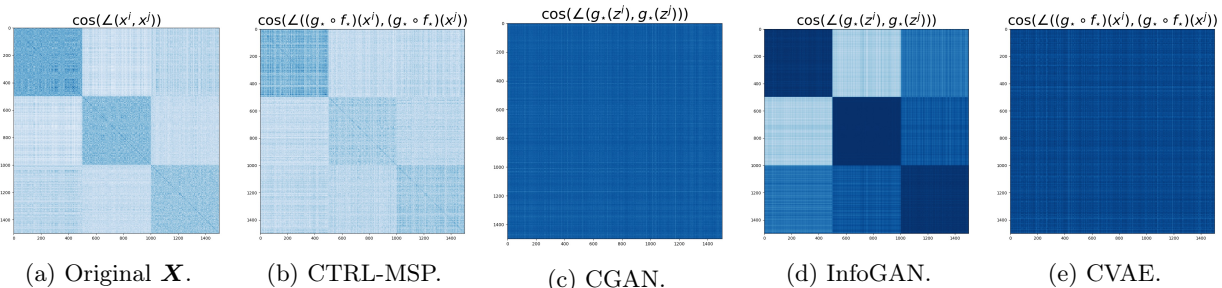


Figure 4: Comparison of generated or reconstructed data correlations.

CTRL-MSP still partially succeeds. Indeed, the cosine similarity heatmap presents a clearly visible block diagonal, the representations corresponding to each subspace \mathcal{S}_j have $d_{\mathcal{S}_j}$ large non-zero singular values, and the subspaces have low projection distance to each other (Figure 3).

4.4 Comparison with Other Representation Learning Methods

We now compare the performance of CTRL-MSG with other supervised representation learning methods, namely Conditional GAN (CGAN) [38], InfoGAN [4], and Conditional VAE (CVAE) [43].⁴ Since these methods do not guarantee discriminative, much less interpretable, representations, we do not compare representations. Instead, we test how well the methods are able to learn the linear structure in the data space, by looking at the correlation structure of the generated or reconstructed data, as in Figure 4. We test $\nu = 0.1$ and $\sigma^2 = 0.01$ as before, train CTRL-MSP for 2 epochs, and all other methods for 1000 epochs; details on all methods used are left to Appendix E.

We observe that InfoGAN and CTRL-MSP attempt to learn the linear structure. CTRL-MSP performs better at detecting separation between subspaces. InfoGAN generally pushes its reconstructions from different subspaces to be correlated, to the point where the first subspace is almost as correlated to the third subspace as it is to itself; which is not seen in CTRL-MSP. Thus, CTRL-MSP learns the linear structure comparably or better than InfoGAN. Meanwhile, CGAN and CVAE degenerate completely, consistent with the theoretical analysis that VAEs may be unable to learn low-dimensional subspaces under certain conditions on the encoder [31]. In summary, the CGAN, InfoGAN, and CVAE architectures use fully nonlinear deep networks and many times the number of training epochs as CTRL-MSP, and yet the latter performs better in the case of low-dimensional subspaces and noise.

⁴The GAN implementations are adapted from PyTorch-GAN [35]; the CVAE implementation is adapted from PyTorch-VAE [44].

5 Generalization via CTRL-SG

We now generalize CTRL-MSP to representation learning scenarios more diverse than our task of learning multiple linear subspace structure. This generalized method, which we call *closed-loop sequential games* (CTRL-SG), builds on sequential game theory and the CTRL framework [6].

Our formulation is inspired by the two roles of the encoder in CTRL, being injective and discriminative with respect to the decoder. Meanwhile, the decoder aims to be compatible with the encoder. We quantify the injectivity of the encoder, which is a boolean value, via the expressiveness—or expansiveness—of the representations, which themselves are quantified by larger values of a function $\mathcal{E}: \mathcal{F} \rightarrow \mathbb{R}$. We quantify the compatibility of the decoder with the encoder via larger values of a function $\mathcal{C}: \mathcal{F} \times \mathcal{G} \rightarrow \mathbb{R}$. We quantify discriminative power of the encoder with respect to the decoder by *lower* values of \mathcal{C} , or alternatively higher values of $-\mathcal{C}$.

These choices are inspired by the GAN framework [1, 18], where the power of the discriminator with respect to the generator is quantified by the difference between the representations of the real and generated data. Similarly, in the CTRL framework, the encoder f seeks to discriminate between the data and the autoencoded data (as well as between each data subspace), by constructing different representations for each. This would mean that the encoder and the decoder are not compatible, so \mathcal{C} would be low and $-\mathcal{C}$ would be high. Thus, the encoder aims to jointly maximize \mathcal{E} and minimize \mathcal{C} ; the decoder aims only to maximize \mathcal{C} . Formalizing this yields the CTRL-SG framework.

Definition 4 (CTRL-SG Game). *The CTRL-SG game is a two-player sequential game between:*

1. *The encoder, moving first, choosing functions f in the function class \mathcal{F} , and having utility function $u_{\text{enc}}(f, g) := \mathcal{E}(f) - \mathcal{C}(f, g)$.*
2. *The decoder, moving second, choosing functions g in the function class \mathcal{G} , and having utility function $u_{\text{dec}}(f, g) := \mathcal{C}(f, g)$.*

Definition 4 is a generalization of Definition 1. More precisely, the CTRL-MSP game is the CTRL-SG game with $\mathcal{F} := \{f \in \mathcal{L}(\mathbb{R}^{d_x}, \mathbb{R}^{d_z}) \mid \|f(\mathbf{X}_j)\|_F^2 \leq n_j \forall j \in \{1, \dots, k\}\}$, $\mathcal{G} := \mathcal{L}(\mathbb{R}^{d_z}, \mathbb{R}^{d_x})$, $\mathcal{E}: f \mapsto \Delta R(f(\mathbf{X}) \mid \mathbf{\Pi})$, and $\mathcal{C}: (f, g) \mapsto -\sum_{j=1}^k \Delta R(f(\mathbf{X}_j), (f \circ g \circ f)(\mathbf{X}_j))$. With these notations, our assumptions are summarized below:

Assumption 5 (Assumptions in CTRL-SG Games).

1. *(Expressiveness can be maximized.) $\arg\max_{f \in \mathcal{F}} \mathcal{E}(f)$ is nonempty.*
2. *(Compatibility can be maximized.) $\arg\max_{g \in \mathcal{G}} \mathcal{C}(f, g)$ is nonempty for every $f \in \mathcal{F}$.*
3. *(The decoder can obtain equally good outcomes regardless of the encoder’s play.) The function $f \mapsto \max_{g \in \mathcal{G}} \mathcal{C}(f, g)$ is constant.*

We may generically characterize the Stackelberg equilibria of CTRL-SG games.

Theorem 6 (Stackelberg Equilibria of CTRL-SG). *If Assumption 5 holds, then the CTRL-SG game has the following properties:*

1. *A Stackelberg equilibrium (f_*, g_*) exists.*
2. *Any Stackelberg equilibrium (f_*, g_*) enjoys:*

$$f_* \in \arg\max_{f \in \mathcal{F}} \mathcal{E}(f), \quad g_* \in \arg\max_{g \in \mathcal{G}} \mathcal{C}(f_*, g).$$

This generalized system allows us to use the CTRL framework for representation learning, to choose principled objective functions to encourage the desired representation, and then to explicitly characterize the optimal learned encoder and decoder for that algorithm. It also suggests principled optimization strategies and algorithms, such as GDMax [24], for obtaining these optimal functions.

This system differs somewhat from the original setting of learning from finite data presented all at once. Since it is a game-theoretic formulation, in principle, one may adapt it to learning contexts different from the ones developed here, e.g., semi-supervised learning and online/incremental learning.

6 Conclusion

In this work, we introduced the closed-loop multi-subspace pursuit (CTRL-MSP) framework for learning representations of the multiple linear subspace structure. We explicitly characterized the Stackelberg equilibria of the associated CTRL-MSP game, and provided empirical support for the proved properties of the learned encoder and decoder. Finally, we introduced a generalization, CTRL-SG, for more general representation learning, and characterized the Stackelberg equilibria of the associated game.

There are several directions for future work. First, the current analysis of CTRL-MSP holds when the data lie perfectly on linear subspaces; it may be fruitful to study the conditions under which the addition of noise causes the learned encoder and decoder for CTRL-MSP to break down or degenerate. Also, it may be interesting to analyze cases where the data lies on more general non-linear manifolds. Regarding CTRL-SG, it is possible to use the framework for other kinds of representation learning problems in different contexts, and characterize the learned encoder and decoder similarly to this work.

In conclusion, CTRL-MSP exemplifies how classical subspace learning problems can be formulated as special cases of modern representation learning problems. In general, unifying classical and modern perspectives greatly contributes towards better understanding the behavior of modern algorithms on both classical and modern problems.

7 Acknowledgements

We thank Peter Tong and Xili Dai of UC Berkeley for insightful discussion regarding practical optimization strategies, as well as fair comparisons to other methods. Edgar would like acknowledge support by the NSF under grants 2046874 and 2031895. Yi would like to acknowledge the support of ONR grants N00014-20-1-2002 and N00014-22-1-2102, the joint Simons Foundation-NSF DMS grant #2031899.

References

- [1] Martin Arjovsky, Soumith Chintala, and Léon Bottou. Wasserstein GAN, 2017. URL <https://arxiv.org/abs/1701.07875>.
- [2] Tamer Başar and Geert Jan Olsder. *Dynamic Noncooperative Game Theory, 2nd Edition*. Society for Industrial and Applied Mathematics, 1998. doi: 10.1137/1.9781611971132. URL <https://epubs.siam.org/doi/abs/10.1137/1.9781611971132>.
- [3] Andreas Buja and Nermin Eyuboglu. Remarks on Parallel Analysis. *Multivariate behavioral research*, 27(4):509–540, 1992.
- [4] Xi Chen, Yan Duan, Rein Houthoofd, John Schulman, Ilya Sutskever, and Pieter Abbeel. Infogan: Interpretable Representation Learning by Information Maximizing Generative Adversarial Nets. *Advances in neural information processing systems*, 29, 2016.
- [5] Thomas M Cover. *Elements of Information Theory*. John Wiley & Sons, 1999.
- [6] Xili Dai, Shengbang Tong, Mingyang Li, Ziyang Wu, Michael Psenka, Kwan Ho Ryan Chan, Pengyuan Zhai, Yaodong Yu, Xiaojun Yuan, Heung-Yeung Shum, and Yi Ma. CTRL: Closed-Loop Transcription to an LDR via Minimizing Rate Reduction. *Entropy*, 24(4), 2022. ISSN 1099-4300. doi: 10.3390/e24040456. URL <https://www.mdpi.com/1099-4300/24/4/456>.
- [7] Constantinos Daskalakis and Ioannis Panageas. Last-Iterate Convergence: Zero-Sum Games and Constrained Min-Max Optimization, 2018. URL <https://arxiv.org/abs/1807.04252>.
- [8] Steven Diamond and Stephen Boyd. CVXPY: A Python-Embedded Modeling Language for Convex Optimization. *Journal of Machine Learning Research*, 17(83):1–5, 2016.
- [9] Edgar Dobriban. Permutation methods for factor analysis and PCA. *The Annals of Statistics*, 48(5): 2824–2847, 2020.

- [10] Edgar Dobriban. Consistency of invariance-based randomization tests. *arXiv preprint arXiv:2104.12260, Annals of Statistics, to appear*, 2021.
- [11] Edgar Dobriban and Art B Owen. Deterministic parallel analysis: an improved method for selecting factors and principal components. *Journal of the Royal Statistical Society. Series B (Methodological)*, 81(1):163–183, 2018.
- [12] William Falcon and The PyTorch Lightning team. PyTorch Lightning, 3 2019. URL <https://github.com/PyTorchLightning/pytorch-lightning>.
- [13] Farzan Farnia and Asuman Ozdaglar. GANs May Have No Nash Equilibria, 2020. URL <https://arxiv.org/abs/2002.09124>.
- [14] Charles Fefferman, Sanjoy Mitter, and Hariharan Narayanan. Testing the Manifold Hypothesis, 2013. URL <https://arxiv.org/abs/1310.0425>.
- [15] Soheil Feizi, Farzan Farnia, Tony Ginart, and David Tse. Understanding GANs: the LQG Setting, 2017. URL <https://arxiv.org/abs/1710.10793>.
- [16] Tanner Fiez, Benjamin Chasnov, and Lillian J. Ratliff. Convergence of Learning Dynamics in Stackelberg Games, 2019. URL <https://arxiv.org/abs/1906.01217>.
- [17] Ian Gemp, Brian McWilliams, Claire Vernade, and Thore Graepel. EigenGame: PCA as a Nash Equilibrium, 2020. URL <https://arxiv.org/abs/2010.00554>.
- [18] Ian J. Goodfellow, Jean Pouget-Abadie, Mehdi Mirza, Bing Xu, David Warde-Farley, Sherjil Ozair, Aaron Courville, and Yoshua Bengio. Generative Adversarial Networks, 2014. URL <https://arxiv.org/abs/1406.2661>.
- [19] Trevor Hastie and Werner Stuetzle. Principal Curves. *Journal of the American Statistical Association*, 84(406):502–516, 1989.
- [20] Zhenliang He, Meina Kan, and Shiguang Shan. EigenGAN: Layer-Wise Eigen-Learning for GANs. In *International Conference on Computer Vision (ICCV)*, 2021.
- [21] David Hong, Yue Sheng, and Edgar Dobriban. Selecting the number of components in PCA via random signflips. *arXiv preprint arXiv:2012.02985*, 2020.
- [22] Harold Hotelling. Analysis of a Complex of Statistical Variables into Principal Components. *Journal of educational psychology*, 24(6):417, 1933.
- [23] He Huang, Philip S. Yu, and Changhu Wang. An Introduction to Image Synthesis with Generative Adversarial Nets, 2018. URL <https://arxiv.org/abs/1803.04469>.
- [24] Chi Jin, Praneeth Netrapalli, and Michael I. Jordan. What is Local Optimality in Nonconvex-Nonconcave Minimax Optimization?, 2019. URL <https://arxiv.org/abs/1902.00618>.
- [25] Ian T Jolliffe. *Principal Component Analysis*. Springer-Verlag, 2nd edition, 2002.
- [26] Olav Kallenberg. *Foundations of Modern Probability*. Probability Theory and Stochastic Modelling. Springer Cham, 2021. ISBN 9783030618704.
- [27] Tero Karras, Samuli Laine, and Timo Aila. A Style-Based Generator Architecture for Generative Adversarial Networks, 2018. URL <https://arxiv.org/abs/1812.04948>.
- [28] Diederik P. Kingma and Jimmy Ba. Adam: A Method for Stochastic Optimization, 2014. URL <https://arxiv.org/abs/1412.6980>.
- [29] Diederik P Kingma and Max Welling. Auto-Encoding Variational Bayes, 2013. URL <https://arxiv.org/abs/1312.6114>.

- [30] Max Kochurov, Rasul Karimov, and Serge Kozlukov. Geopt: Riemannian Optimization in PyTorch, 2020. URL <https://arxiv.org/abs/2005.02819>.
- [31] Frederic Koehler, Viraj Mehta, Andrej Risteski, and Chenghui Zhou. Variational Autoencoders in the Presence of Low-dimensional Data: Landscape and Implicit Bias. *arXiv preprint arXiv:2112.06868*, 2021.
- [32] Mark A Kramer. Nonlinear principal component analysis using autoassociative neural networks. *AICHE journal*, 37(2):233–243, 1991.
- [33] Yenson Lau, Qing Qu, Han-Wen Kuo, Pengcheng Zhou, Yuqian Zhang, and John Wright. Short and Sparse Deconvolution — A Geometric Approach. In *International Conference on Learning Representations*, 2020. URL <https://openreview.net/forum?id=Byg5ZANtvH>.
- [34] Yanjun Li and Yoram Bresler. Global Geometry of Multichannel Sparse Blind Deconvolution on the Sphere. In *Advances in Neural Information Processing Systems*, pages 1132–1143, 2018.
- [35] Erik Linder-Norén. PyTorch-GAN. <https://github.com/eriklindernoren/PyTorch-GAN>, 2018.
- [36] Yi Ma, Harm Derksen, Wei Hong, and John Wright. Segmentation of Multivariate Mixed Data via Lossy Data Coding and Compression. *IEEE Transactions on Pattern Analysis and Machine Intelligence*, 29(9):1546–1562, 2007. doi: 10.1109/TPAMI.2007.1085.
- [37] Ajkel Mino and Gerasimos Spanakis. LoGAN: Generating Logos with a Generative Adversarial Neural Network Conditioned on color, 2018. URL <https://arxiv.org/abs/1810.10395>.
- [38] Mehdi Mirza and Simon Osindero. Conditional Generative Adversarial Nets. *arXiv preprint arXiv:1411.1784*, 2014.
- [39] Adam Paszke, Sam Gross, Francisco Massa, Adam Lerer, James Bradbury, Gregory Chanan, Trevor Killeen, Zeming Lin, Natalia Gimelshein, Luca Antiga, Alban Desmaison, Andreas Köpf, Edward Yang, Zach DeVito, Martin Raison, Alykhan Tejani, Sasank Chilamkurthy, Benoit Steiner, Lu Fang, Junjie Bai, and Soumith Chintala. PyTorch: An Imperative Style, High-Performance Deep Learning Library, 2019. URL <https://arxiv.org/abs/1912.01703>.
- [40] Vignesh Prasad, Dipanjan Das, and Brojeshwar Bhowmick. Variational Clustering: Leveraging Variational Autoencoders for Image Clustering. *arXiv*, 2020. doi: 10.48550/ARXIV.2005.04613. URL <https://arxiv.org/abs/2005.04613>.
- [41] Qing Qu, Yuexiang Zhai, Xiao Li, Yuqian Zhang, and Zhihui Zhu. Geometric Analysis of Nonconvex Optimization Landscapes for Overcomplete Learning. In *International Conference on Learning Representations*, 2019.
- [42] Yifei Shen, Ye Xue, Jun Zhang, Khaled B Letaief, and Vincent Lau. Complete Dictionary Learning via ℓ_p -norm Maximization. *arXiv preprint arXiv:2002.10043*, 2020.
- [43] Kihyuk Sohn, Honglak Lee, and Xinchen Yan. Learning Structured Output Representation using Deep Conditional Generative Models. In C. Cortes, N. Lawrence, D. Lee, M. Sugiyama, and R. Garnett, editors, *Advances in Neural Information Processing Systems*, volume 28. Curran Associates, Inc., 2015. URL <https://proceedings.neurips.cc/paper/2015/file/8d55a249e6baa5c06772297520da2051-Paper.pdf>.
- [44] A.K Subramanian. PyTorch-VAE. <https://github.com/AntixK/PyTorch-VAE>, 2020.
- [45] Michael E Tipping and Christopher M Bishop. Probabilistic Principal Component Analysis. *Journal of the Royal Statistical Society: Series B (Statistical Methodology)*, 61(3):611–622, 1999.
- [46] Shengbang Tong, Xili Dai, Ziyang Wu, Mingyang Li, Brent Yi, and Yi Ma. Incremental Learning of Structured Memory via Closed-Loop Transcription, 2022. URL <https://arxiv.org/abs/2202.05411>.

- [47] Laurens Van Der Maaten, Eric Postma, and Jaap Van den Herik. Dimensionality Reduction: a Comparative. *J Mach Learn Res*, 10(66-71):13, 2009.
- [48] Rene Vidal, Yi Ma, and Shankar Sastry. Generalized Principal Component Analysis (GPCA). *arXiv*, 2012. doi: 10.48550/ARXIV.1202.4002. URL <https://arxiv.org/abs/1202.4002>.
- [49] René Vidal, Yi Ma, and Shankar Sastry. *Generalized Principal Component Analysis*. Springer Verlag, 2016.
- [50] John Wright and Yi Ma. *High-Dimensional Data Analysis with Low-Dimensional Models: Principles, Computation, and Applications*. Cambridge University Press, 2022.
- [51] Yaodong Yu, Kwan Ho Ryan Chan, Chong You, Chaobing Song, and Yi Ma. Learning Diverse and Discriminative Representations via the Principle of Maximal Coding Rate Reduction, 2020. URL <https://arxiv.org/abs/2006.08558>.
- [52] Yuexiang Zhai, Hermish Mehta, Zhengyuan Zhou, and Yi Ma. Understanding ℓ_4 -based Dictionary Learning: Interpretation, Stability, and Robustness. In *International Conference on Learning Representations*, 2019.
- [53] Yuexiang Zhai, Zitong Yang, Zhenyu Liao, John Wright, and Yi Ma. Complete Dictionary Learning via ℓ_4 -Norm Maximization over the Orthogonal Group. *J. Mach. Learn. Res.*, 21(165):1–68, 2020.
- [54] Yuqian Zhang, Han-Wen Kuo, and John Wright. Structured Local Optima in Sparse Blind Deconvolution. *IEEE Transactions on Information Theory*, 66(1):419–452, 2019.
- [55] Banghua Zhu, Jiantao Jiao, and David Tse. Deconstructing generative adversarial networks. *IEEE Transactions on Information Theory*, 66(11):7155–7179, 2020.

Appendix

The appendix is organized as follows. In Appendix A we discuss the mathematical and information-theoretic foundations of rate reduction theory. In Appendix B we discuss popular representation learning algorithms, such as PCA, GAN, and CTRL in terms of simultaneous game theory and the representation learning framework we developed. In Appendix C we give proofs of all theorems in the main body. In Appendix D we discuss a specialization of CTRL-MSP, which we call CTRL-SSP, to the case where the data lies on a single linear subspace; in this section we give mathematical justification and empirical support for CTRL-SSP. In Appendix E we provide more experimental details, a more thorough empirical evaluation of CTRL-MSP, and more detailed comparisons with other representation learning algorithms.

A Rate Reduction Functions

In this section, we discuss the rate reduction functions from Section 2.2, and provide more details on the rate reduction schema. Much of the exposition is motivated by [36, 51]. The perspective will be information-theoretic; basics of information theory are covered in [5].

Let $\mathbf{z} \in \mathbb{R}^{d_z}$ be a random vector, and let $\text{RD}(\cdot | \mathbf{z})$ be the rate distortion function of \mathbf{z} with respect to the Euclidean squared distance distortion. Information-theoretically, this is a measure of the *coding rate* of the data; that is, the average number of bits required to encode \mathbf{z} , such that the expected Euclidean squared distance between \mathbf{z} and its encoding is at most the argument of the function.

For a symmetric matrix \mathbf{A} , let $\lambda_{\min}(\mathbf{A})$ be the minimum eigenvalue of \mathbf{A} . If $\mathbf{u} \sim \mathcal{N}(\mathbf{0}_{d_z}, \mathbf{\Gamma})$ is a multivariate Gaussian random vector with mean $\mathbf{0}_{d_z}$ and covariance $\mathbf{\Gamma}$, then

$$\text{RD}(\varepsilon | \mathbf{u}) = \frac{1}{2} \log_2 \det \left(\frac{d_z}{\varepsilon^2} \mathbf{\Gamma} \right) \quad \forall \varepsilon \in [0, \sqrt{d_z \cdot \lambda_{\min}(\mathbf{\Gamma})}].$$

For larger ε , the rate distortion function becomes more complicated and can be found by the water-filling algorithm on the eigenvalues of $\mathbf{\Gamma}$. However, [36] proposes the following approximation of the rate distortion. For $\mathbf{w}_\varepsilon \sim \mathcal{N}\left(\mathbf{0}_{d_z}, \frac{\varepsilon^2}{d_z} \mathbf{I}_{d_z}\right)$ independent of \mathbf{z} , let

$$R_\varepsilon(\mathbf{z}) := \text{RD}(\varepsilon \mid \mathbf{z} + \mathbf{w}_\varepsilon).$$

If $\mathbf{z} \sim \mathcal{N}(\mathbf{0}_{d_z}, \mathbf{\Sigma})$, then we may derive a closed form expression for $R_\varepsilon(\mathbf{z})$ for *all* $\varepsilon > 0$. Since \mathbf{z} and \mathbf{w}_ε are normally distributed, so is $\mathbf{z} + \mathbf{w}_\varepsilon$, and

$$\mathbf{z} + \mathbf{w}_\varepsilon \sim \mathcal{N}\left(\mathbf{0}_{d_z}, \frac{\varepsilon^2}{d_z} \mathbf{I}_{d_z} + \mathbf{\Sigma}\right).$$

Thus,

$$\sqrt{d_z \cdot \lambda_{\min}\left(\frac{\varepsilon^2}{d_z} \mathbf{I}_{d_z} + \mathbf{\Sigma}\right)} = \sqrt{d_z \cdot \left(\frac{\varepsilon^2}{d_z} + \lambda_{\min}(\mathbf{\Sigma})\right)} = \sqrt{\varepsilon^2 + d_z \lambda_{\min}(\mathbf{\Sigma})} \geq \varepsilon.$$

Therefore, we have the following closed form expression for $R_\varepsilon(\mathbf{z})$ for *all* $\varepsilon > 0$.

$$R_\varepsilon(\mathbf{z}) = \text{RD}(\varepsilon \mid \mathbf{z} + \mathbf{w}_\varepsilon) = \frac{1}{2} \log_2 \det\left(\frac{d_z}{\varepsilon^2} \left(\mathbf{\Sigma} + \frac{\varepsilon^2}{d_z} \mathbf{I}_{d_z}\right)\right) = \frac{1}{2} \log_2 \det\left(\mathbf{I}_{d_z} + \frac{d_z}{\varepsilon^2} \mathbf{\Sigma}\right).$$

In information-theoretic terms, $R_\varepsilon(\mathbf{z})$ is a *regularized rate distortion* measure, and corresponds to the expansiveness of the distribution of \mathbf{z} .

From this measure we can also define a measure of difference⁵ between distributions of two possibly-correlated random vectors $\mathbf{z}_1, \mathbf{z}_2 \in \mathbb{R}^{d_z}$. This measure estimates the average number of bits saved by encoding \mathbf{z}_1 and \mathbf{z}_2 separately and independently compared to encoding them together, say by encoding a mixture random variable \mathbf{z} which is \mathbf{z}_1 with probability $\frac{1}{2}$ and \mathbf{z}_2 with probability $\frac{1}{2}$. In this notation, we have

$$\Delta R_\varepsilon(\mathbf{z}_1, \mathbf{z}_2) := R_\varepsilon(\mathbf{z}) - \frac{1}{2} R_\varepsilon(\mathbf{z}_1) - \frac{1}{2} R_\varepsilon(\mathbf{z}_2).$$

This measure of difference has several advantages over Wasserstein or Jensen-Shannon distances. It is a principled measure of difference which is computable in closed-form for the widely representative class of Gaussian distributions. In particular, due to the existence of the closed-form representation, it is much simpler to do analysis on the solutions of optimization problems involving these measures.

We may generalize the difference measure to several random vectors. Specifically, define probabilities $\pi_1, \dots, \pi_k \in [0, 1]$ such that $\sum_{j=1}^k \pi_j = 1$, arranged in a vector $\boldsymbol{\pi} \in [0, 1]^k$, and let $\mathbf{z}_1, \dots, \mathbf{z}_k \in \mathbb{R}^{d_z}$ be random vectors. Define \mathbf{z} to be the mixture random vector which equals \mathbf{z}_j with probability π_j . Then the *coding rate reduction* is given by

$$\Delta R_\varepsilon(\mathbf{z} \mid \boldsymbol{\pi}) := R_\varepsilon(\mathbf{z}) - \sum_{j=1}^k \pi_j R_\varepsilon(\mathbf{z}_j).$$

This is a measure of how expansive the distribution of each \mathbf{z}_j is, and how different the distributions of the \mathbf{z}_j are from each other – in some sense, the expressiveness and discriminativeness of the distributions of the \mathbf{z}_j . More precisely, it was shown in [51] that, subject to rank and Frobenius norm constraints on the \mathbf{z}_j , this expression is maximized when the \mathbf{z}_j are distributed on pairwise orthogonal subspaces, and also each \mathbf{z}_j has isotropic (or nearly isotropic) covariance on its subspace.

In practice, we do not know the distribution of the data, and the features are not perfectly a mixture of Gaussians. Still, the mixture of Gaussians is often a reasonable model for lower-dimensional feature distributions [6, 36, 51], so we use the Gaussian form for the approximate coding rate.

Also, in practice we do not have access to any full distributions, and so we need to estimate all relevant quantities via a finite sample. For Gaussians, R_ε is only a function of \mathbf{z} through its covariance $\mathbf{\Sigma}$; in practice, this covariance is estimated via a finite sample $\mathbf{Z} \in \mathbb{R}^{d_z \times n}$ as $\mathbf{Z}\mathbf{Z}^\top/n$. This also allows us to estimate

⁵This measure is not a true distance function; for starters, this measure can be zero for random variables with non-identical distributions.

$\Delta R_\varepsilon(\cdot, \cdot)$ from a finite sample. To estimate $\Delta R_\varepsilon(\cdot | \cdot)$, we also need to estimate $\boldsymbol{\pi}$. For this, we require finite sample information $\boldsymbol{\Pi}$ telling us which samples correspond to which random vector \mathbf{z}_j . Denote by $n_j \geq 1$ the number of samples in \mathcal{Z} which correspond to \mathbf{z}_j . Then $\boldsymbol{\pi}$ may be estimated via plug-in as $\hat{\pi}_j = \frac{n_j}{n}$.

This set of approximations yields estimates $R_\varepsilon(\mathcal{Z})$, $\Delta R_\varepsilon(\mathcal{Z}_1, \mathcal{Z}_2)$, and $\Delta R_\varepsilon(\mathcal{Z} | \boldsymbol{\Pi})$, whose expressions for Gaussians are given in Section 2.2 (dropping the ε subscript and working in the natural logarithm instead of the base-2 logarithm).

B PCA, GAN, CTRL as Games

In the main body of the paper, we use the framework of learning an encoder function $f \in \mathcal{F}$ and decoder function $g \in \mathcal{G}$ via a two-player *sequential* game between the encoder and decoder. This is different than conventional formulations of other representation learning algorithms, including PCA, nonlinear PCA (autoencoding) [32], GANs [1, 18], and CTRL [6] as *simultaneous* games between the encoder (or discriminator) and decoder (or generator). For completeness, we briefly introduce aspects of simultaneous game theory (a more detailed introduction is again found in [2]), and then discuss each of these frameworks in terms of our general representation learning formulation as well as simultaneous game theory.

Simultaneous Game Theory. In a simultaneous game between the encoder — playing $f \in \mathcal{F}$ — and the decoder — playing $g \in \mathcal{G}$ — both players make their move at the same time with no information about the other player’s move. As in the sequential game framework, both players rationally attempt to maximize their utility functions $u_{\text{enc}}: \mathcal{F} \times \mathcal{G} \rightarrow \mathbb{R}$ and $u_{\text{dec}}: \mathcal{F} \times \mathcal{G} \rightarrow \mathbb{R}$ respectively. The solution concept for a simultaneous game is a so-called *Nash equilibrium*. Formally, $(f_\star, g_\star) \in \mathcal{F} \times \mathcal{G}$ is a Nash equilibrium if and only if

$$f_\star \in \operatorname{argmax}_{f \in \mathcal{F}} u_{\text{enc}}(f, g_\star), \quad g_\star \in \operatorname{argmax}_{g \in \mathcal{G}} u_{\text{dec}}(f, g_\star).$$

PCA and Autoencoding. PCA finds the best approximating subspace, which we denote \mathcal{S}_{PCA} , to the data in the following sense. Let $\text{Gr}(d_z, \mathbb{R}^{d_x})$ be the set of d_z -dimensional linear subspaces of \mathbb{R}^{d_x} . Then, PCA solves the problem

$$\mathcal{S}_{\text{PCA}} \in \operatorname{argmin}_{S \in \text{Gr}(d_z, \mathbb{R}^{d_x})} \sum_{i=1}^n \|\mathbf{x}^i - \text{proj}_S(\mathbf{x}^i)\|_{\ell^2}^2.$$

The solution is well-known and exists in closed form in terms of the SVD of the data matrix \mathbf{X} [50]. To formulate this problem in terms of a game between an encoder and decoder, we learn the orthogonal projection operator $\text{proj}_S(\cdot)$ as a rank- d_z composition of so-called *semi-orthogonal* linear maps. Let $p, q \geq 1$ be integers. For a linear map $h: \mathbb{R}^p \rightarrow \mathbb{R}^q$ denote its transpose $h^\top: \mathbb{R}^q \rightarrow \mathbb{R}^p$ as the linear map whose matrix representation is the transpose of the matrix representation of h . For a set A let $\text{id}_A: A \rightarrow A$ be the identity map on A . Finally, define the semi-orthogonal linear maps $\text{O}(\mathbb{R}^p, \mathbb{R}^q)$ by

$$\text{O}(\mathbb{R}^p, \mathbb{R}^q) := \left\{ h \in \mathcal{L}(\mathbb{R}^p, \mathbb{R}^q) \mid \begin{array}{l} h^\top \circ h = \text{id}_{\mathbb{R}^p} \quad \text{if } p \leq q \\ h \circ h^\top = \text{id}_{\mathbb{R}^q} \quad \text{if } q \leq p \end{array} \right\}.$$

We may then define a PCA game to learn the projection operator.

Definition 7 (PCA Game). *The PCA game is a two-player simultaneous game between:*

1. *The encoder, choosing functions f in the function class $\mathcal{F} := \text{O}(\mathbb{R}^{d_x}, \mathbb{R}^{d_z})$, and having utility function $u_{\text{enc}}(f, g) := -\sum_{i=1}^n \|\mathbf{x}^i - (g \circ f)(\mathbf{x}^i)\|_{\ell^2}$.*
2. *The decoder, choosing functions g in the function class $\mathcal{G} := \text{O}(\mathbb{R}^{d_z}, \mathbb{R}^{d_x})$, and having utility function $u_{\text{dec}}(f, g) := -\sum_{i=1}^n \|\mathbf{x}^i - (g \circ f)(\mathbf{x}^i)\|_{\ell^2}$.*

There are alternate formulations of PCA as a game [17].

Autoencoder games [32] may be formulated similar to PCA games, perhaps with the same utility functions, but the function classes \mathcal{F} and \mathcal{G} are less constrained. In particular, they may include functions modelled by neural networks. This makes the Nash point analysis much more difficult.

GANs. In the GAN framework [1, 18], f is interpreted as a discriminator and g is interpreted as a generator. Unlike the cooperative games of PCA and autoencoding, GANs train the generator and discriminator functions adversarially, in a zero-sum fashion (meaning $u_{\text{enc}} = -u_{\text{dec}}$). The generator attempts to fool the discriminator to treat generated data similarly to real data (by mapping to similar representations), while the discriminator seeks to discriminate between real data and generated data. Let $\mathbf{Z} \in \mathbb{R}^{d_z \times n}$ be a random matrix whose entries are i.i.d. (probably Gaussian) noise. Also, let $d: \mathbb{R}^{d_x \times n} \times \mathbb{R}^{d_x \times n} \rightarrow \mathbb{R}$ be any finite-sample estimate of the distance between the distributions which generate the columns of its first argument and second argument (for the purpose of concreteness, one may take d to be an estimator of the Jensen-Shannon divergence or Wasserstein distance). Then the GAN training game may be posited as follows.

Definition 8 (GAN Game). *The GAN game is a two-player simultaneous game between:*

1. *The discriminator, choosing functions f in the function class \mathcal{F} , and having utility function $u_{\text{enc}}(f, g) := d(f(\mathbf{X}), (g \circ f)(\mathbf{Z}))$.*
2. *The generator, choosing functions g in the function class \mathcal{G} , and having utility function $u_{\text{dec}}(f, g) := -d(f(\mathbf{X}), (g \circ f)(\mathbf{Z}))$.*

Despite having conceptually simple foundations, GANs have technical problems. The above two-player game may not have a Nash equilibrium [13], and even \mathcal{F} and \mathcal{G} are very simple, e.g., linear and quadratic functions, and one assumes that equilibria exists, GANs may not converge to the equilibria [15]. A further, very important, complexity is that the distances most commonly used for GANs, such as Wasserstein distance and Jensen-Shannon divergence [1], are defined variationally and do not have a closed form for any non-trivial distributions (even mixtures of Gaussians). Thus, one has to approximate the distance via another distance function which is more tractable [1]; this estimate becomes worse as the data dimension increases [50].

CTRL. In CTRL [6], the function f is both an encoder and a discriminator, while g is both a decoder and generator. Closed-loop training compares the representations $f(\mathbf{X})$ and the representations of the autoencoded data $(f \circ g \circ f)(\mathbf{X})$. More specifically, using the rate reduction difference measure $\Delta R(\cdot, \cdot)$ discussed in Section 2.2 and expanded on more in Appendix A, the difference measure between the distributions generating the representations of the data and of the autoencoded data is estimated by the class-wise difference measure $\sum_{j=1}^k \Delta R(f(\mathbf{X}_j), (f \circ g \circ f)(\mathbf{X}_j))$. Similar to the GAN game, the encoder attempts to maximize this quantity, and the decoder attempts to minimize it. Unlike the GAN game, CTRL also wants to achieve structured representations; in order to do this, the encoder jointly attempts to maximize the representation expressiveness and discriminativeness of both the data and the autoencoded data, which is represented by an additive term $\Delta R(f(\mathbf{X}) | \mathbf{\Pi}) + \Delta R((f \circ g \circ f)(\mathbf{X}) | \mathbf{\Pi})$. Formalizing this gives the CTRL game.

Definition 9 (CTRL Game). *The CTRL game is a two-player simultaneous game between:*

1. *The encoder, choosing functions f in the function class \mathcal{F} , and having utility function*

$$u_{\text{enc}}(f, g) := \Delta R(f(\mathbf{X}) | \mathbf{\Pi}) + \Delta R((f \circ g \circ f)(\mathbf{X}) | \mathbf{\Pi}) + \sum_{j=1}^k \Delta R(f(\mathbf{X}_j), (f \circ g \circ f)(\mathbf{X}_j)).$$

2. *The decoder, choosing functions f in the function class \mathcal{F} , and having utility function $u_{\text{dec}}(f, g) := -u_{\text{enc}}(f, g)$.*

Theoretical analysis of this particular simultaneous game is still an open problem, though this formulation [6] and other closely related formulations [46] have achieved good empirical results.

C Proofs of Theorem 6 and Theorem 3

We prove the result from Section 5 first, then we show that it specializes to the result in Section 3.

C.1 Proof of Theorem 6

Proof. We show both consequences of the theorem at the same time, by first computing the equilibria f_* , then computing the corresponding g_* . By assumption 5.3, the function $f \mapsto \max_{g \in \mathcal{G}} \mathcal{C}(f, g)$ is constant; say equal to $c \in \mathbb{R}$. Then we have

$$\begin{aligned} & \operatorname{argmax}_{f \in \mathcal{F}} \inf \left\{ u_{\text{enc}}(f, g) \mid g \in \operatorname{argmax}_{\tilde{g} \in \mathcal{G}} u_{\text{dec}}(f, \tilde{g}) \right\} \\ &= \operatorname{argmax}_{f \in \mathcal{F}} \inf \left\{ \mathcal{E}(f) - \mathcal{C}(f, g) \mid g \in \operatorname{argmax}_{\tilde{g} \in \mathcal{G}} \mathcal{C}(f, \tilde{g}) \right\} \\ &= \operatorname{argmax}_{f \in \mathcal{F}} \left[\mathcal{E}(f) - \sup \left\{ \mathcal{C}(f, g) \mid g \in \operatorname{argmax}_{\tilde{g} \in \mathcal{G}} \mathcal{C}(f, \tilde{g}) \right\} \right] \\ &= \operatorname{argmax}_{f \in \mathcal{F}} \left[\mathcal{E}(f) - \max_{g \in \mathcal{G}} \mathcal{C}(f, g) \right] = \operatorname{argmax}_{f \in \mathcal{F}} [\mathcal{E}(f) - c] = \operatorname{argmax}_{f \in \mathcal{F}} \mathcal{E}(f). \end{aligned}$$

By assumption 5.1, this set is nonempty. Suppose f_* is in this set. Then

$$\operatorname{argmax}_{g \in \mathcal{G}} u_{\text{dec}}(f_*, g) = \operatorname{argmax}_{g \in \mathcal{G}} \mathcal{C}(f_*, g)$$

and by assumption 5.2, this set is also nonempty. Thus, a Stackelberg equilibrium exists. If (f_*, g_*) is a Stackelberg equilibrium, then $f_* \in \operatorname{argmax}_{f \in \mathcal{F}} \mathcal{E}(f)$ by the first calculation, and $g_* \in \operatorname{argmax}_{g \in \mathcal{G}} \mathcal{C}(f_*, g)$ by the second calculation, confirming the remaining part of the theorem. \square

C.2 Proof of Theorem 3

The proof of this theorem is split up into several steps, which we capture into a few lemmas.

1. We first show that the CTRL-MSP game is a particular instance of the CTRL-SG game. We show that if the CTRL-MSP assumptions hold then the CTRL-SG assumptions hold.
2. We then characterize the optima of the expressiveness and compatibility functions of the CTRL-MSP game.

Lemma 10. *The CTRL-MSP game is an instance of the CTRL-SG game. Moreover, if the CTRL-MSP assumptions hold then the CTRL-SG assumptions hold.*

Proof. The CTRL-MSP game is an instance of the CTRL-SG game, with the following correspondences:

- $\mathcal{F} := \{f \in \mathcal{L}(\mathbb{R}^{d_x}, \mathbb{R}^{d_z}) \mid \|f(\mathbf{X}_j)\|_F^2 \leq n_j \forall j \in \{1, \dots, k\}\}$.
- $\mathcal{G} := \mathcal{L}(\mathbb{R}^{d_z}, \mathbb{R}^{d_x})$.
- $\mathcal{E}: f \mapsto \Delta R(f(\mathbf{X}) \mid \mathbf{\Pi})$.
- $\mathcal{C}: (f, g) \mapsto -\sum_{j=1}^k \Delta R(f(\mathbf{X}_j), (f \circ g \circ f)(\mathbf{X}_j))$.

We now show that the CTRL-SG assumptions hold. First, we claim that the set $\operatorname{argmax}_{f \in \mathcal{F}} \mathcal{E}(f) = \operatorname{argmax}_{f \in \mathcal{F}} \Delta R(f(\mathbf{X}) \mid \mathbf{\Pi})$ is nonempty. Let $\mathcal{S} := \operatorname{Span}\left(\bigcup_{j=1}^k \mathcal{S}_j\right)$. While \mathcal{E} is continuous in f , compactness (required for the usual argument showing the existence of maxima) is not immediate from the definition: linear maps in \mathcal{F} are controlled only on \mathcal{S} and may have arbitrarily large operator norms on \mathcal{S}^\perp , thus making \mathcal{F} an unbounded set and not compact. To remedy this, consider the related problem of optimization over the set

$$\mathcal{F}' := \mathcal{F} \cap \{f \in \mathcal{L}(\mathbb{R}^{d_x}, \mathbb{R}^{d_z}) \mid f(\mathcal{S}^\perp) = \{\mathbf{0}\}\}.$$

Now we have $\max_{f \in \mathcal{F}} \mathcal{E}(f) = \max_{f \in \mathcal{F}'} \mathcal{E}(f)$ and $\operatorname{argmax}_{f \in \mathcal{F}'} \mathcal{E}(f) \subseteq \operatorname{argmax}_{f \in \mathcal{F}} \mathcal{E}(f)$. Thus, it suffices to show that $\operatorname{argmax}_{f \in \mathcal{F}'} \mathcal{E}(f)$ is nonempty. Clearly \mathcal{F}' is compact. The extreme value theorem holds for optimizing \mathcal{E} over \mathcal{F}' , and the claim is proved.

Now we claim that $\operatorname{argmax}_{g \in \mathcal{G}} \mathcal{C}(f, g) = \operatorname{argmin}_{g \in \mathcal{G}} \sum_{j=1}^k \Delta R(f(\mathbf{X}_j), (f \circ g \circ f)(\mathbf{X}_j))$ exists for every f . Indeed, Lemma A.4 from [51] shows that $\Delta R(\mathbf{Z}_1, \mathbf{Z}_2) \geq 0$ with equality if and only if $\mathbf{Z}_1 \mathbf{Z}_1^\top = \mathbf{Z}_2 \mathbf{Z}_2^\top$, so $\mathcal{C}(f, g) \leq 0$ for all $(f, g) \in \mathcal{F} \times \mathcal{G}$. If f^+ is taken to be the Moore-Penrose pseudoinverse of f , then $f \circ f^+ \circ f = f$ and $\mathcal{C}(f, f^+) = 0$, which implies $f^+ \in \operatorname{argmax}_{g \in \mathcal{G}} \mathcal{C}(f, g)$. This implies that the set of maximizers is nonempty, proving the claim.

Finally, we claim that the function $f \mapsto \max_{g \in \mathcal{G}} \mathcal{C}(f, g)$ is constant. Indeed, by the choice of $g = f^+$ which is well-defined for all linear maps f , this function is constantly zero, as desired. \square

Now, we can separate the utility and analyze its parts; this is the main theoretical benefit of casting the problem in the CTRL-SG paradigm.

Lemma 11. *Suppose the CTRL-MSP assumptions hold, and let \mathcal{F}, \mathcal{G} be defined as in the CTRL-MSP game. Then any $f_\star \in \operatorname{argmax}_{f \in \mathcal{F}} \Delta R(f(\mathbf{X}) \mid \mathbf{\Pi})$ enjoys properties 2a&b from Theorem 3.*

Proof. First, since $f_\star \in \mathcal{F}$ is linear, $f_\star(\mathcal{S}_j)$ is a linear subspace; further, $\dim(f_\star(\mathcal{S}_j)) \leq d_{\mathcal{S}_j}$. We now claim that the subspaces $\{f_\star(\mathcal{S}_j)\}_{j=1}^k$ are orthogonal. Since $f_\star(\mathcal{S}_j) = \operatorname{Col}(f_\star(\mathbf{X}_j))$, this is equivalent to the columns of $f_\star(\mathbf{X}_j)$ being orthogonal to the columns of $f_\star(\mathbf{X}_\ell)$ for all $\ell \neq j$, i.e., $f_\star(\mathbf{X}_j)^\top f_\star(\mathbf{X}_\ell) = \mathbf{0}$.

The essential tool we use to show that the $f_\star(\mathbf{X}_j)$ have orthogonal columns is Lemma A.5 of [51], which states that, for matrices $\mathbf{Z}_j \in \mathbb{R}^{d_z \times n_j}$ which are collected in a matrix $\mathbf{Z} \in \mathbb{R}^{d_z \times n}$,

$$\Delta R(\mathbf{Z} \mid \mathbf{\Pi}) \leq \frac{1}{2n} \sum_{j=1}^k \sum_{p=1}^{d_{\mathcal{S}_j}} \log \left(\frac{\left(1 + \frac{d_z}{n \varepsilon^2} \sigma_p(\mathbf{Z}_j)^2\right)^n}{\left(1 + \frac{d_z}{n_j \varepsilon^2} \sigma_p(\mathbf{Z}_j)^2\right)^{n_j}} \right) \quad (1)$$

with equality if and only if $\mathbf{Z}_j^\top \mathbf{Z}_\ell = 0$ for all $1 \leq j < \ell \leq k$.

Suppose for the sake of contradiction that $f_\star(\mathbf{X}_j)^\top f_\star(\mathbf{X}_\ell) \neq \mathbf{0}$ for some $1 \leq j < \ell \leq k$. Since $d_z \geq \sum_{j=1}^k d_{\mathcal{S}_j}$ and the subspaces \mathcal{S}_j , $j = 1, \dots, k$ have linearly independent bases, one can construct via the SVD another linear map $\tilde{f} \in \mathcal{L}(\mathbb{R}^{d_x}, \mathbb{R}^{d_z})$ such that

- $\sigma_p(f_\star(\mathbf{X}_j)) = \sigma_p(\tilde{f}(\mathbf{X}_j))$, for $1 \leq p \leq d_{\mathcal{S}_j}$ and $1 \leq j \leq k$.
- $\tilde{f}(\mathbf{X}_j)^\top \tilde{f}(\mathbf{X}_\ell) = 0$ for all for $1 \leq j < \ell \leq k$.

Then for each j we have

$$\left\| \tilde{f}(\mathbf{X}_j) \right\|_F^2 = \sum_{p=1}^{d_{\mathcal{S}_j}} \sigma_p^2(\tilde{f}(\mathbf{X}_j)) = \sum_{p=1}^{d_{\mathcal{S}_j}} \sigma_p^2(f_\star(\mathbf{X}_j)) = \|f_\star(\mathbf{X}_j)\|_F^2 \leq n_j$$

so we have $\tilde{f} \in \mathcal{F}$. Further, since equality holds in the inequality (1) of Lemma A.5 of [51] for \tilde{f} but not for f_\star , we have

$$\begin{aligned} \Delta R(\tilde{f}(\mathbf{X}) \mid \mathbf{\Pi}) &= \frac{1}{2n} \sum_{j=1}^k \sum_{p=1}^{d_{\mathcal{S}_j}} \log \left(\frac{\left(1 + \frac{d_z}{n \varepsilon^2} \sigma_p(\tilde{f}(\mathbf{X}_j))^2\right)^n}{\left(1 + \frac{d_z}{n_j \varepsilon^2} \sigma_p(\tilde{f}(\mathbf{X}_j))^2\right)^{n_j}} \right) \\ &= \frac{1}{2n} \sum_{j=1}^k \sum_{p=1}^{d_{\mathcal{S}_j}} \log \left(\frac{\left(1 + \frac{d_z}{n \varepsilon^2} \sigma_p(f_\star(\mathbf{X}_j))^2\right)^n}{\left(1 + \frac{d_z}{n_j \varepsilon^2} \sigma_p(f_\star(\mathbf{X}_j))^2\right)^{n_j}} \right) > \Delta R(f_\star(\mathbf{X}) \mid \mathbf{\Pi}). \end{aligned}$$

Thus f_\star does not maximize $f \mapsto \Delta R(f(\mathbf{X}) \mid \mathbf{\Pi})$ over $f \in \mathcal{F}$, a contradiction. Thus, we must have that $f_\star(\mathbf{X}_j)^\top f_\star(\mathbf{X}_\ell) = \mathbf{0}$ for all $1 \leq j < \ell \leq k$, and so the $\{f_\star(\mathcal{S}_j)\}_{j=1}^k$ are orthogonal subspaces.

Now, we claim that either $\sigma_1(f_\star(\mathbf{X}_j)) = \dots = \sigma_{d_{\mathcal{S}_j}}(f_\star(\mathbf{X}_j)) = \frac{n_j}{d_j}$, or $\sigma_1(f_\star(\mathbf{X}_j)) = \dots = \sigma_{d_{\mathcal{S}_j}-1}(f_\star(\mathbf{X}_j)) \in (\frac{n_j}{d_j}, \frac{n_j}{d_j-1})$ and $\sigma_{d_{\mathcal{S}_j}}(f_\star(\mathbf{X}_j)) > 0$. To show this, the general approach is to isolate the effect of f_\star on each \mathbf{X}_j . In particular, fix $t \in \{1, \dots, k\}$. We claim that

$$f_\star \in \operatorname{argmax}_{f \in \mathcal{F}} \sum_{p=1}^{d_{\mathcal{S}_t}} \log \left(\frac{\left(1 + \frac{d_z}{n \varepsilon^2} \sigma_p(f(\mathbf{X}_t))^2\right)^n}{\left(1 + \frac{d_z}{n_t \varepsilon^2} \sigma_p(f(\mathbf{X}_t))^2\right)^{n_t}} \right). \quad (2)$$

Indeed, suppose that this does not hold, and there exists $\hat{f} \in \mathcal{F}$ such that

$$\sum_{p=1}^{d_{\mathcal{S}_t}} \log \left(\frac{\left(1 + \frac{d_z}{n\varepsilon^2} \sigma_p(f_\star(\mathbf{X}_t))^2\right)^n}{\left(1 + \frac{d_z}{n_t\varepsilon^2} \sigma_p(f_\star(\mathbf{X}_t))^2\right)^{n_t}} \right) < \sum_{p=1}^{d_{\mathcal{S}_t}} \log \left(\frac{\left(1 + \frac{d_z}{n\varepsilon^2} \sigma_p(\hat{f}(\mathbf{X}_t))^2\right)^n}{\left(1 + \frac{d_z}{n_t\varepsilon^2} \sigma_p(\hat{f}(\mathbf{X}_t))^2\right)^{n_t}} \right).$$

Then, again since $d_z \geq \sum_{j=1}^k d_{\mathcal{S}_j}$ and the subspaces \mathcal{S}_j have linearly independent bases, one can construct another linear map $\tilde{f} \in \mathcal{L}(\mathbb{R}^{d_x}, \mathbb{R}^{d_z})$ such that

- $\sigma_p(\tilde{f}(\mathbf{X}_t)) = \sigma_p(\hat{f}(\mathbf{X}_t))$, for $1 \leq p \leq d_{\mathcal{S}_t}$.
- $\sigma_p(\tilde{f}(\mathbf{X}_j)) = \sigma_p(f_\star(\mathbf{X}_j))$, for $1 \leq p \leq d_{\mathcal{S}_j}$, $1 \leq j \leq k$ with $j \neq t$.
- $\tilde{f}(\mathbf{X}_j)^\top \tilde{f}(\mathbf{X}_\ell) = \mathbf{0}$ for $1 \leq j < \ell \leq k$.

For the same reason as in the previous claim, $\tilde{f} \in \mathcal{F}$. Moreover, $\Delta R(\tilde{f}(\mathbf{X}) \mid \mathbf{\Pi}) > \Delta R(f_\star(\mathbf{X}) \mid \mathbf{\Pi})$, because

$$\begin{aligned} & 2n \cdot \Delta R(\tilde{f}(\mathbf{X}) \mid \mathbf{\Pi}) \\ &= \sum_{p=1}^{d_{\mathcal{S}_t}} \log \left(\frac{\left(1 + \frac{d_z}{n\varepsilon^2} \sigma_p(\tilde{f}(\mathbf{X}_t))^2\right)^n}{\left(1 + \frac{d_z}{n_t\varepsilon^2} \sigma_p(\tilde{f}(\mathbf{X}_t))^2\right)^{n_t}} \right) + \sum_{\substack{j=1 \\ j \neq t}}^k \sum_{p=1}^{d_{\mathcal{S}_j}} \log \left(\frac{\left(1 + \frac{d_z}{n\varepsilon^2} \sigma_p(\tilde{f}(\mathbf{X}_j))^2\right)^n}{\left(1 + \frac{d_z}{n_j\varepsilon^2} \sigma_p(\tilde{f}(\mathbf{X}_j))^2\right)^{n_j}} \right) \\ &= \sum_{p=1}^{d_{\mathcal{S}_t}} \log \left(\frac{\left(1 + \frac{d_z}{n\varepsilon^2} \sigma_p(\hat{f}(\mathbf{X}_t))^2\right)^n}{\left(1 + \frac{d_z}{n_t\varepsilon^2} \sigma_p(\hat{f}(\mathbf{X}_t))^2\right)^{n_t}} \right) + \sum_{\substack{j=1 \\ j \neq t}}^k \sum_{p=1}^{d_{\mathcal{S}_j}} \log \left(\frac{\left(1 + \frac{d_z}{n\varepsilon^2} \sigma_p(f_\star(\mathbf{X}_j))^2\right)^n}{\left(1 + \frac{d_z}{n_j\varepsilon^2} \sigma_p(f_\star(\mathbf{X}_j))^2\right)^{n_j}} \right). \end{aligned}$$

This is strictly lower bounded by

$$\begin{aligned} & \sum_{p=1}^{d_{\mathcal{S}_t}} \log \left(\frac{\left(1 + \frac{d_z}{n\varepsilon^2} \sigma_p(f_\star(\mathbf{X}_t))^2\right)^n}{\left(1 + \frac{d_z}{n_t\varepsilon^2} \sigma_p(f_\star(\mathbf{X}_t))^2\right)^{n_t}} \right) + \sum_{\substack{j=1 \\ j \neq t}}^k \sum_{p=1}^{d_{\mathcal{S}_j}} \log \left(\frac{\left(1 + \frac{d_z}{n\varepsilon^2} \sigma_p(f_\star(\mathbf{X}_j))^2\right)^n}{\left(1 + \frac{d_z}{n_j\varepsilon^2} \sigma_p(f_\star(\mathbf{X}_j))^2\right)^{n_j}} \right) \\ &= 2n \cdot \Delta R(f_\star(\mathbf{X}) \mid \mathbf{\Pi}). \end{aligned}$$

Thus f_\star is not a maximizer of $f \mapsto \Delta R(f(\mathbf{X}) \mid \mathbf{\Pi})$, which is a contradiction. Hence, (2) follows.

To finish, we may now solve the problem in terms of the singular values of $f(\mathbf{X}_t)$. Indeed, from the above optimization problem and the definition of \mathcal{F} , the singular values $\sigma_p(f_\star(\mathbf{X}_t))$ are the solutions of the scalar optimization problem

$$\max_{\sigma_1, \dots, \sigma_{d_{\mathcal{S}_t}} \in \mathbb{R}} \sum_{p=1}^{d_{\mathcal{S}_t}} \log \left(\frac{\left(1 + \frac{d_z}{n\varepsilon^2} \sigma_p^2\right)^n}{\left(1 + \frac{d_z}{n_t\varepsilon^2} \sigma_p^2\right)^{n_t}} \right) \quad \text{s.t.} \quad \sigma_1 \geq \dots \geq \sigma_{d_{\mathcal{S}_t}} \geq 0, \quad \sum_{p=1}^{d_{\mathcal{S}_t}} \sigma_p^2 = n_j.$$

Given the assumption that ε is small enough, Lemma A.7 of [51] says that the solutions to this optimization problem either fulfill $\sigma_1 = \dots = \sigma_{d_{\mathcal{S}_t}} = \frac{n_j}{d_{\mathcal{S}_t}}$ or $\sigma_1 = \dots = \sigma_{d_{\mathcal{S}_t}-1} \in \left(\frac{n_t}{d_{\mathcal{S}_t}}, \frac{n_t}{d_{\mathcal{S}_t}-1}\right)$ and $\sigma_{d_{\mathcal{S}_t}} > 0$ as desired, where if $d_{\mathcal{S}_t} = 1$ then $\frac{n_t}{d_{\mathcal{S}_t}-1}$ is interpreted as $+\infty$. This also confirms that $\dim(f_\star(\mathcal{S}_t)) = \text{rank}(f_\star(\mathbf{X}_t)) = d_{\mathcal{S}_t}$. \square

We now characterize the maximizers of the compatibility function.

Lemma 12. *Suppose the CTRL-MSP assumptions hold, and let \mathcal{F}, \mathcal{G} be defined as in the CTRL-MSP game. Let $f_\star \in \mathcal{F}$. Then for any $g_\star \in \text{argmin}_{g \in \mathcal{G}} \sum_{j=1}^k \Delta R(f_\star(\mathbf{X}_j), (f_\star \circ g_\star \circ f_\star)(\mathbf{X}_j))$, we have property 2c from Theorem 3.*

Proof. From Lemma A.4 of [51], we have $\Delta R(\mathbf{Z}_1, \mathbf{Z}_2) \geq 0$ with equality if and only if $\mathbf{Z}_1 \mathbf{Z}_1^\top = \mathbf{Z}_2 \mathbf{Z}_2^\top$. Picking $g \in \mathcal{G}$ to be the pseudoinverse f_\star^+ of f_\star shows that $f_\star = f_\star \circ f_\star^+ \circ f_\star = f_\star \circ g \circ f_\star$, implying that $\sum_{j=1}^k \Delta R(f_\star(\mathbf{X}_j), (f_\star \circ g \circ f_\star)(\mathbf{X}_j)) = 0$. Thus $\text{argmin}_{g \in \mathcal{G}} \sum_{j=1}^k \Delta R(f_\star(\mathbf{X}_j), (f_\star \circ g \circ f_\star)(\mathbf{X}_j))$ is exactly the

set of $g_\star \in \mathcal{G}$ such that $\sum_{j=1}^k \Delta R(f_\star(\mathbf{X}_j), (f_\star \circ g_\star \circ f_\star)(\mathbf{X}_j)) = 0$. Indeed, this means that, for each j , we have $f_\star(\mathbf{X}_j)f_\star(\mathbf{X}_j)^\top = (f_\star \circ g_\star \circ f_\star)(\mathbf{X}_j)(f_\star \circ g_\star \circ f_\star)(\mathbf{X}_j)^\top$. This implies there exists a matrix \mathbf{W}_j such that $f_\star(\mathbf{X}_j) = (f_\star \circ g_\star \circ f_\star)(\mathbf{X}_j) \cdot \mathbf{W}_j$. Thus, $\text{Col}(f_\star(\mathbf{X}_j)) = \text{Col}((f_\star \circ g_\star \circ f_\star)(\mathbf{X}_j))$. The former is exactly $f_\star(\mathcal{S}_j)$, and the latter term is $(f_\star \circ g_\star \circ f_\star)(\mathcal{S}_j)$, so equality holds and the lemma is proved. \square

With Lemmas 10 to 12, we are now able to cleanly prove Theorem 3.

Proof of Theorem 3. By Lemma 10 and Theorem 6, we have that, if the CTRL-MSP assumptions hold, a Stackelberg equilibrium to the CTRL-MSP game exists, and that any Stackelberg equilibrium (f_\star, g_\star) enjoys:

$$f_\star \in \operatorname{argmax}_{f \in \mathcal{F}} \Delta R(f(\mathbf{X}) \mid \mathbf{\Pi}), \quad g_\star \in \operatorname{argmin}_{g \in \mathcal{G}} \sum_{j=1}^k \Delta R(f_\star(\mathbf{X}_j), (f_\star \circ g \circ f_\star)(\mathbf{X}_j)).$$

By Lemmas 11 and 12, the conclusions all follow. \square

D Single-Subspace Pursuit via the CTRL Framework

D.1 Theory of CTRL-SSP

We may specialize the CTRL-SG framework to obtain a method for *single subspace pursuit*, called CTRL-SSP, which has similar properties to PCA. Suppose in our notation that $k = 1$, so that $\mathbf{X}_1 = \mathbf{X}$. We drop the subscript on the only linear subspace \mathcal{S}_1 which supports the data, to obtain the single data subspace \mathcal{S} with dimension $d_{\mathcal{S}}$.

Our formulation of PCA in Appendix B as finding the best subspace of dimension d_z for the data shows that, if $d_z \geq d_{\mathcal{S}}$ then $\mathcal{S}_{\text{PCA}} \supseteq \mathcal{S}$. Thus $g_{\text{PCA}} \circ f_{\text{PCA}}$ is the identity on \mathcal{S} , so the semi-orthogonal linear maps f_{PCA} and g_{PCA} must be isometries on \mathcal{S} and $f_{\text{PCA}}(\mathcal{S})$ respectively. This isometric property is the essential property of the PCA encoder we choose to achieve in CTRL-SSP; our encoder must preserve all distances and thus all the structure of the subspace.

To present the CTRL-SSP game, recall the definition of $\mathcal{O}(\cdot, \cdot)$ from Appendix B.

Definition 13 (CTRL-SSP Game). *The CTRL-SSP game is a two-player sequential game between:*

1. *The encoder, moving first, choosing functions f in the function class $\mathcal{F} := \mathcal{O}(\mathbb{R}^{d_x}, \mathbb{R}^{d_z})$ and having utility function $u_{\text{enc}}(f, g) := R(f(\mathbf{X})) + \Delta R(f(\mathbf{X}), (f \circ g \circ f)(\mathbf{X}))$.*
2. *The decoder, moving second, choosing functions g in the function class $\mathcal{G} := \mathcal{O}(\mathbb{R}^{d_z}, \mathbb{R}^{d_x})$, and having utility function $u_{\text{dec}}(f, g) := -\Delta R(f(\mathbf{X}), (f \circ g \circ f)(\mathbf{X}))$.*

Assumption 14 (Assumptions in CTRL-SSP Games).

1. *(Informative data.)* $\text{Col}(\mathbf{X}) = \mathcal{S}$.
2. *(Large enough representation space.)* $d_{\mathcal{S}} \leq \min\{d_x, d_z\}$.

We may now explicitly characterize the Stackelberg equilibria of CTRL-SSP.

Theorem 15 (Stackelberg Equilibria of CTRL-SSP Games). *If Assumption 14 holds, then the CTRL-SSP game has the following properties:*

1. *A Stackelberg equilibrium (f_\star, g_\star) exists.*
2. *Any Stackelberg equilibrium (f_\star, g_\star) enjoys the following properties:*
 - (a) *(Injective encoder.)* $f_\star(\mathcal{S})$ is a linear subspace of dimension $d_{\mathcal{S}}$, and f_\star is an ℓ^2 -isometry on \mathcal{S} .
 - (b) *(Consistent encoding and decoding.)* $f_\star(\mathcal{S}) = (f_\star \circ g_\star \circ f_\star)(\mathcal{S})$.

The proof of this theorem is split up into several steps, similarly to the CTRL-SSP picture.

1. We first show that the CTRL-SSP game is a particular instance of the CTRL-SG game. We show that if the CTRL-SSP assumptions hold then the CTRL-SG assumptions hold.
2. We then characterize the optima of the expressiveness and compatibility functions of the CTRL-SSP game.

Lemma 16. *The CTRL-SSP game is an instance of the CTRL-SG game. Moreover, if the CTRL-SSP assumptions hold then the CTRL-SG assumptions hold.*

Proof. One may easily see that the CTRL-SSP game is an instance of the CTRL-SG game, with the following correspondences:

- $\mathcal{F} := \mathcal{O}(\mathbb{R}^{d_x}, \mathbb{R}^{d_z})$.
- $\mathcal{G} := \mathcal{O}(\mathbb{R}^{d_z}, \mathbb{R}^{d_x})$.
- $\mathcal{E}: f \mapsto R(f(\mathbf{X}))$.
- $\mathcal{C}: (f, g) \mapsto -\Delta R(f(\mathbf{X}), (f \circ g \circ f)(\mathbf{X}))$.

We show that the CTRL-SG assumptions hold. We first claim that $\operatorname{argmax}_{f \in \mathcal{F}} \mathcal{E}(f) = \operatorname{argmax}_{f \in \mathcal{F}} R(f(\mathbf{X}))$ is nonempty. Indeed, \mathcal{F} is compact and \mathcal{E} is continuous in f , so the conclusion follows by the extreme value theorem. Further, using the same argument as in the corresponding part of the proof of lemma 10, for every $f \in \mathcal{F}$, we have that $\operatorname{argmax}_{g \in \mathcal{G}} \mathcal{C}(f, g) = \operatorname{argmin}_{g \in \mathcal{G}} \Delta R(f(\mathbf{X}), (f \circ g \circ f)(\mathbf{X}))$ is nonempty. We finally claim that the function $f \mapsto \max_{g \in \mathcal{G}} \mathcal{C}(f, g)$ is constant. Indeed, by the choice of $g = f^+$, which for $f \in \mathcal{F} = \mathcal{O}(\mathbb{R}^{d_x}, \mathbb{R}^{d_z})$ is contained in $\mathcal{G} = \mathcal{O}(\mathbb{R}^{d_z}, \mathbb{R}^{d_x})$, this function is constantly zero, as desired. \square

Again, we can separate the utility and analyze each part of it.

Lemma 17. *Suppose the CTRL-SSP assumptions hold, and let \mathcal{F}, \mathcal{G} be defined as in the CTRL-SSP game. Then any $f_\star \in \operatorname{argmax}_{f \in \mathcal{F}} R(f(\mathbf{X}))$ enjoys property 2a from theorem 15.*

Proof. Since f_\star is a linear map and \mathcal{S} is a linear subspace, $f_\star(\mathcal{S})$ is a linear subspace, and furthermore $\dim(f_\star(\mathcal{S})) \leq d_{\mathcal{S}}$. We now claim that f_\star is an ℓ^2 -isometry on \mathcal{S} . We show this by calculating an upper bound for $R(f(\mathbf{X}))$ and show that it is achieved if and only if f is an ℓ^2 -isometry on \mathcal{S} .

Indeed, for any $f \in \mathcal{F} = \mathcal{O}(\mathbb{R}^{d_x}, \mathbb{R}^{d_z})$, we have that f has operator norm and Lipschitz constant equal to unity, so $\|f(\mathbf{x})\|_{\ell^2} \leq \|\mathbf{x}\|_{\ell^2}$ for any $\mathbf{x} \in \mathbb{R}^{d_x}$. By the Courant-Fischer min-max theorem for singular values, we have, for each $1 \leq p \leq d_{\mathcal{S}}$,

$$\sigma_p(f(\mathbf{X})) = \sup_{S \in \operatorname{Gr}(p, \mathbb{R}^{d_x})} \inf_{\substack{\mathbf{u} \in S \\ \|\mathbf{u}\|_{\ell^2} = 1}} \|f(\mathbf{X}) \cdot \mathbf{u}\|_{\ell^2} \leq \sup_{S \in \operatorname{Gr}(p, \mathbb{R}^{d_x})} \inf_{\mathbf{u} \in S, \|\mathbf{u}\|_{\ell^2} = 1} \|\mathbf{X} \cdot \mathbf{u}\|_{\ell^2} = \sigma_p(\mathbf{X}).$$

Thus

$$\begin{aligned} R(f(\mathbf{X})) &= \frac{1}{2} \log \det \left(\mathbf{I}_{d_z} + \frac{d_z}{n\varepsilon^2} f(\mathbf{X}) f(\mathbf{X})^\top \right) \\ &= \frac{1}{2} \sum_{p=1}^{d_{\mathcal{S}}} \log \left(1 + \frac{d_z}{n\varepsilon^2} \sigma_p(f(\mathbf{X}))^2 \right) \leq \frac{1}{2} \sum_{p=1}^{d_{\mathcal{S}}} \log \left(1 + \frac{d_z}{n\varepsilon^2} \sigma_p(\mathbf{X})^2 \right). \end{aligned}$$

Clearly, f is an ℓ^2 isometry on \mathcal{S} if and only if $\sigma_p(f(\mathbf{X})) = \sigma_p(\mathbf{X})$ for all $1 \leq p \leq d_{\mathcal{S}}$. Thus, any $f_\star \in \mathcal{F}$ which fulfills the upper bound for $R(f(\mathbf{X}))$, i.e., any maximizer for $R(f(\mathbf{X}))$, is an ℓ^2 isometry on \mathcal{S} . Therefore, clearly $\dim(f_\star(\mathcal{S})) = d_{\mathcal{S}}$. \square

Lemma 18. *Suppose the CTRL-SSP assumptions hold, and let \mathcal{F}, \mathcal{G} be defined as in the CTRL-SSP game. Let $f_\star \in \operatorname{argmax}_{f \in \mathcal{F}} R(f(\mathbf{X}))$. Then any $g_\star \in \operatorname{argmin}_{g \in \mathcal{G}} \Delta R(f(\mathbf{X}), (f \circ g \circ f)(\mathbf{X}))$ enjoys property 2b from theorem 15.*

Proof. The proof is exactly as the proof of Lemma 12, and is thus omitted. \square

With Lemmas 16 to 18, we are now able to prove Theorem 15.

Proof of Theorem 15. The proof is exactly as the proof of Theorem 3, and is thus omitted. \square

D.2 Empirical Evidence for CTRL-SSP

We now present some further experiments for the CTRL-SSP framework on single subspaces. Throughout these experiments in various settings, we are primarily concerned with the following metrics:

1. The *spectrum of the data matrix* \mathbf{X} , which may be viewed as representing the complexity of the dataset.
2. The *spectrum of the representation matrix* $f_*(\mathbf{X})$, which demonstrates the expressiveness of the learned encoding map f_* on the data \mathbf{X} by way of representing the complexity of the learned representations $f_*(\mathbf{X})$. We want the singular values of $f_*(\mathbf{X})$ to be as close to the singular values of \mathbf{X} as possible, so as to demonstrate the isometric property of f_* .
3. The *isometry ratios* $\frac{\|f_*(\mathbf{x}^i) - f_*(\mathbf{x}^j)\|_{\ell^2}}{\|\mathbf{x}^i - \mathbf{x}^j\|_{\ell^2}}$ for all data point pairs $\mathbf{x}^i, \mathbf{x}^j \in \mathbf{X}, i \neq j$, to measure closeness of f_* to an isometry on \mathbf{X} . These values are collected in a histogram, which is ideally concentrated close to unity if f_* is near-isometric on \mathbf{X} .
4. The *subspace alignment* $\text{Resid}(f_*(\mathbf{X}), \text{Col}(f_*(\mathbf{X}), f_*(g_*(f_*(\mathbf{X}))))$, which is the set of projection residuals $\left\| f_*(\mathbf{x}^i) - \text{proj}_{\text{Col}(f_*(g_*(f_*(\mathbf{X})))}(f_*(\mathbf{x}^i)) \right\|_{\ell^2}$ for every i . This measures the closeness of the subspaces spanned by the columns of $f_*(\mathbf{X})$ and $f_*(g_*(f_*(\mathbf{X})))$ by way of computing the projection residuals. These values are collected in a histogram, which is ideally concentrated close to 0 if $\text{Col}(f_*(\mathbf{X})) = \text{Col}(f_*(g_*(f_*(\mathbf{X}))))$.

For each experiment, we present graphs of the above four metrics. Each experiment will be a variation from a baseline setting to demonstrate the performance of CTRL-SSP with respect to important properties of the underlying problem (dimension of X , noise, etc.).

The baseline settings are given by the following: $n = 500, d_x = 50, d_z = 40, d_S = 10, \sigma^2 = 0.0$, and $\varepsilon^2 = 1$. For further experiments comparing with GAN and VAE, those architectures are identical: 10 layer FCNN encoder, 10 layer FCNN decoder, latent/noise dimension is 40 for VAE/GAN, and each hidden layer has 100 dimensions. See Section 4 for information on the data generation process (for which we set $\nu = 0$ in this section), and Appendix E for further details on our experimental setup, with the additional caveat that we use `GeoOpt` [30] for optimization over $O(\cdot, \cdot)$.

In Figures 5 to 11, we present results for multiple experimental settings. Of important note is the consistency for the measured metrics when we both (a) scale the embedding/intrinsic dimensions, and (b) introduce noise in the data. Principled ways to choose the subspace dimension for PCA could be used in the noisy setting [3, 9, 10, 11, 21].

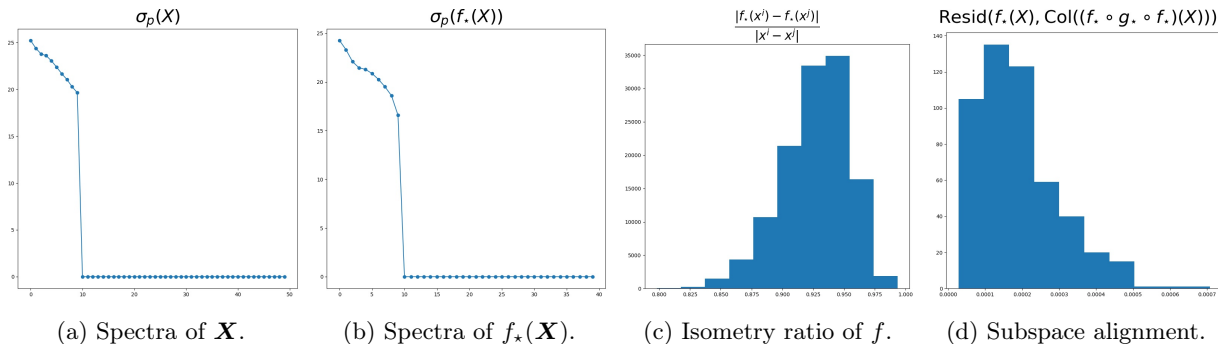


Figure 5: Baseline behavior of CTRL-SSP. Refer to the introductory paragraphs of this section (Appendix D.2) for details on the presented graphs.

E Additional Empirical Evidence and Comparisons

Our experiments use PyTorch [39] and PyTorch Lightning [12]. Our comparisons with GANs use implementations from PyTorch-GAN [35], and our comparisons with VAEs use implementations from PyTorch-VAE

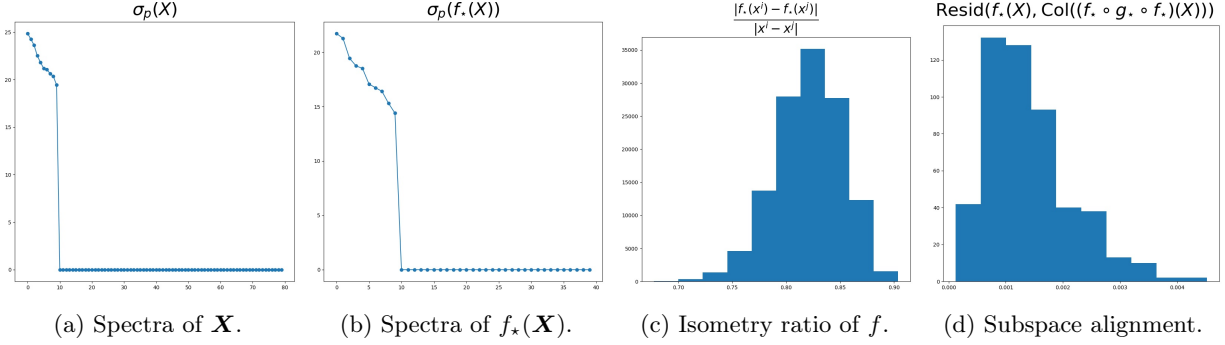


Figure 6: Behavior of CTRL-SSP with $d_x = 80$ (larger than baseline). Of important note is the similarity to Fig. 5; the resulting representation only depends on the intrinsic dimension rather than the extrinsic dimension.

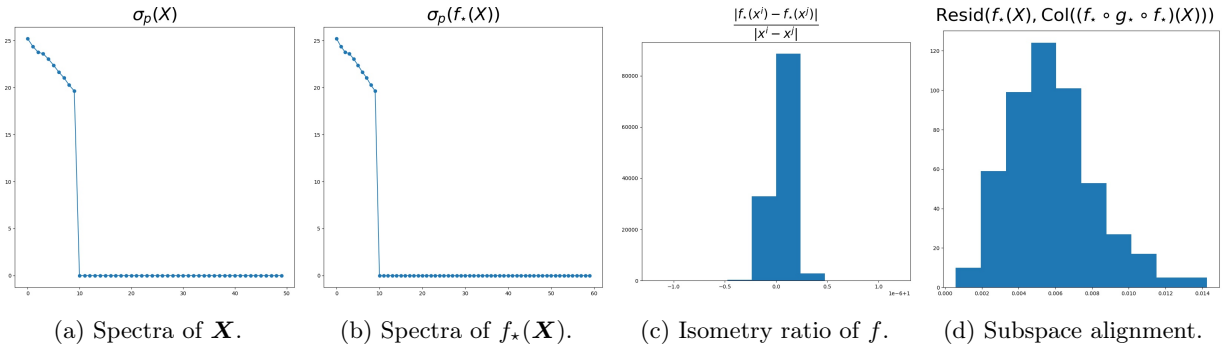


Figure 7: Behavior of CTRL-SSP with $d_z = 60$ (larger than baseline). As we increase the size of the representation space, the learning problem becomes “better conditioned”: resulting representations have more regular spectra, and desired isometry/alignment properties become easier to obtain.

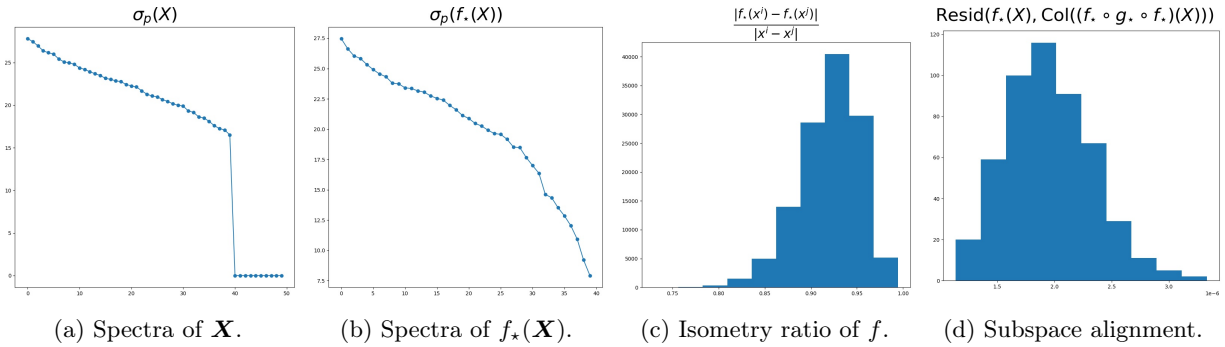


Figure 8: Behavior of CTRL-SSP when $d_S = d_z = 40$ (increase in d_S). As we increase the intrinsic dimension of the data to the theoretical maximum that the representation space (z -space) can manage, CTRL-SSP remains a tractable algorithmic framework to find a viable representation.

[44].⁶ Our implementations are in general adapted to learn vector data instead of image data, which most original implementations are written for. Our experiments are run on a 2018 MacBook Pro with a 2.2 GHz 6-Core Intel Core i7 and 16 GB of DDR4 RAM at 2400 MHz. The code to run the experiments is stored at the [linked GitHub repository](#).

The optimization method we use is stochastic projected GDMax [24], which can be described as follows:

⁶Both libraries have permissive enough licenses (MIT and Apache 2.0, respectively) for us to use variations of their code.

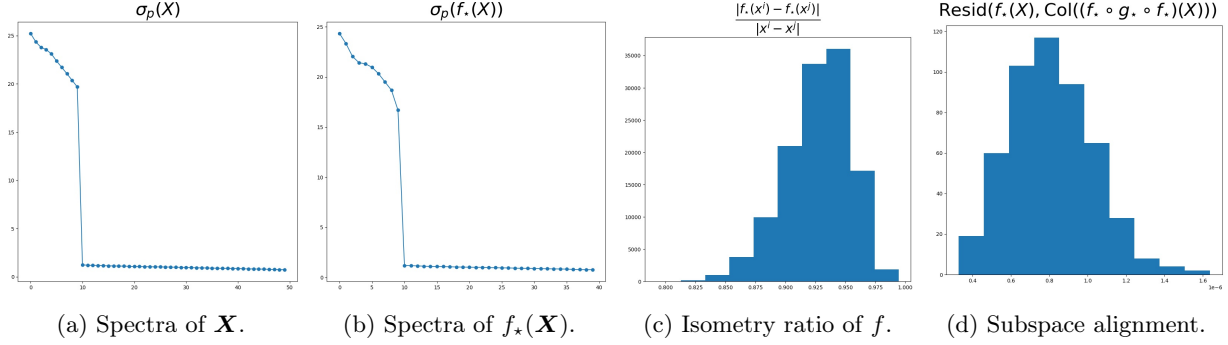


Figure 9: Behavior of CTRL-SSP when adding Gaussian noise with uniform variance $\sigma^2 = 0.1$. Note that we still observe ideal isometry and reconstruction properties.

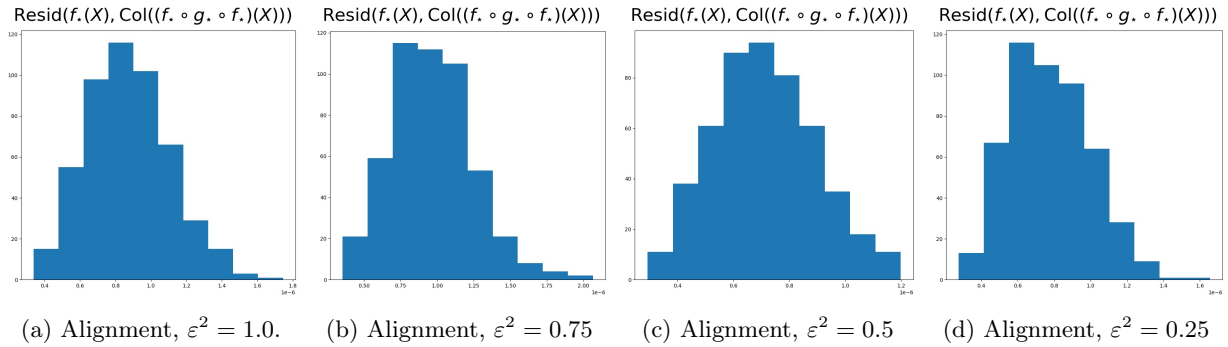


Figure 10: Behavior of CTRL-SSP for varying ε^2 given $\sigma^2 = 0.01$. In contrast to the experiments of [36], we do not observe a phase transition phenomenon when increasing the ε^2 parameter for the rate reduction functions.

- Run one iteration of gradient descent on f to maximize $u_{\text{enc}}(f, g) = \Delta R(f(\mathbf{X}) \mid \mathbf{\Pi}) + \sum_{j=1}^k \Delta R(f(\mathbf{X}_j), (f \circ g \circ f)(\mathbf{X}_j))$. The gradient descent has learning rate 10^{-2} .
- Project f onto \mathcal{F} using `cvxpy` [8].
- Run gradient descent on g to minimize $u_{\text{dec}}(f, g) = \sum_{j=1}^k \Delta R(f(\mathbf{X}_j), (f \circ g \circ f)(\mathbf{X}_j))$ until convergence. The gradient descent has learning rate 10^{-3} .
- Repeat from the first step until f converges or time horizon is reached.

In practice, instead of waiting for the convergence of g , we run gradient descent on g for 10^3 iterations; instead of waiting for convergence of f , we optimize f for two epochs. We also use Adam [28] instead of pure gradient descent, with the default PyTorch hyperparameters other than the specified learning rate. This leads to accelerated convergence, though preliminary experiments indicate that regular gradient descent learns the same equilibria with a somewhat larger number of epochs, say 5 instead of 2.

Throughout our experiments in various settings, we are primarily concerned with the following metrics:

1. The *spectrum of the data matrices* \mathbf{X}_j and the *spectrum of the representation matrices* $f_*(\mathbf{X}_j)$, for the same reasons as before. This time, we would like the top $d_{\mathcal{S}_j}$ singular values of $f_*(\mathbf{X}_j)$ to be large and nonzero.
2. The *pairwise absolute cosine similarity of the columns of the data matrix* \mathbf{X} , which represents the initial coherence of the data.
3. The *pairwise absolute cosine similarity of the columns of the representation matrix* $f_*(\mathbf{X})$, which demonstrates the discriminativeness of the learned encoding map f_* on the data by way of representing

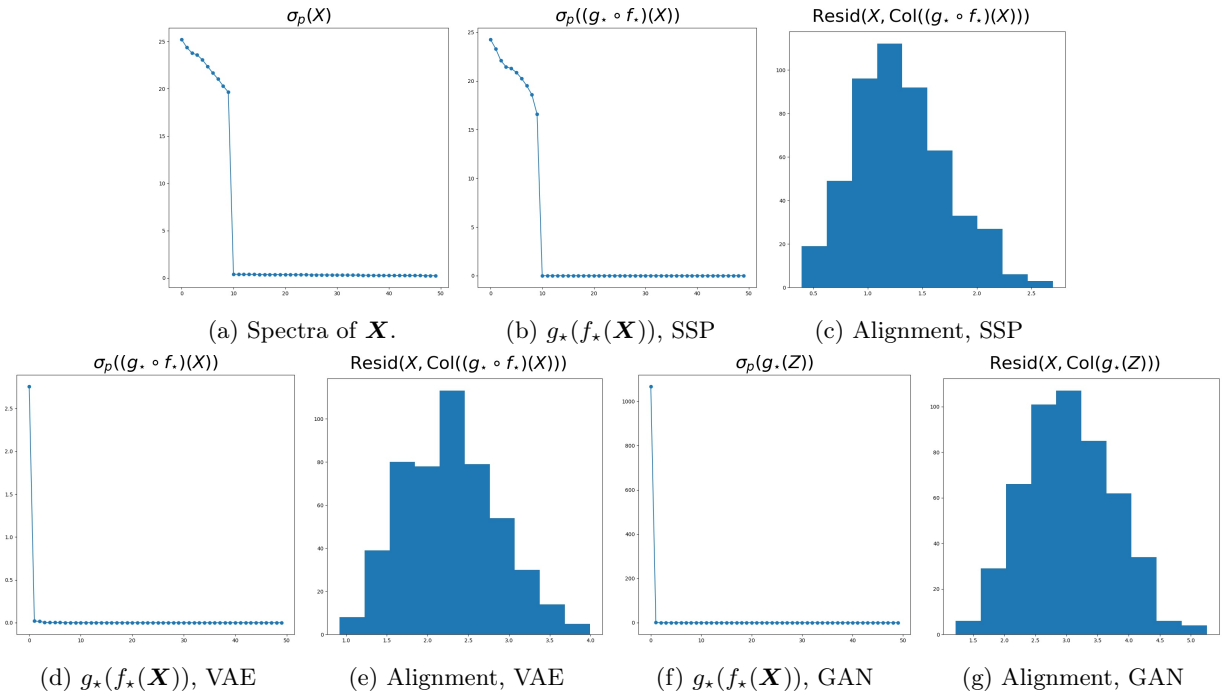


Figure 11: Comparisons with various representation learning methods: CTRL-SSP (ours, labeled SSP in figures), VAE, and GAN. Note that these standard GAN and VAE have no explicit promoters of diverse representations, and thus their learnt representations are overcompressed and one-dimensional. Additionally, their alignment scores are marginally worse.

the coherence of the learned representations $f_*(\mathbf{X})$. Since our data in \mathbf{X} is sorted by class, we want the heatmap of pairwise absolute cosine similarities to have block diagonal structure, indicating strong intra-class coherence and inter-class incoherence.

4. The *subspace alignments* $\text{Resid}(f_*(\mathbf{X}_j), \text{Col}(f_*(g_*(f_*(\mathbf{X}_j))))$, for the same reasons as before.

The baseline settings are given by the following: $k = 3$, $n = 1500$, $n_1 = n_2 = n_3 = n/k = 500$, $d_x = 50$, $d_z = 40$, $d_{S_1} = 3$, $d_{S_2} = 4$, $d_{S_3} = 5$, $\sigma^2 = 0$, and $\varepsilon^2 = 1$. The data generation process is given in Section 4; for "benign" subspaces we take $\nu = 10^6$, while for "coherent" subspaces we take $\nu = 0.1$. For further experiments when we compare with GAN and VAE variants, their architectures are identical, and are as in Appendix D.2, with the caveat that InfoGAN has an additional parameter, the so-called "code dimension" d_{code} , which we set to 20.

In Figures 12-16, we provide results for multiple experimental settings, all for benign subspaces. Of particular note is the phase transition behavior of the performance when adding more noise, and the robustness of the performance to different values of ε . In Figures 17-21, we provide extremely similar results for coherent subspaces, showing that the initial correlations between subspaces truly does not affect the inherent difficulty of the problem.

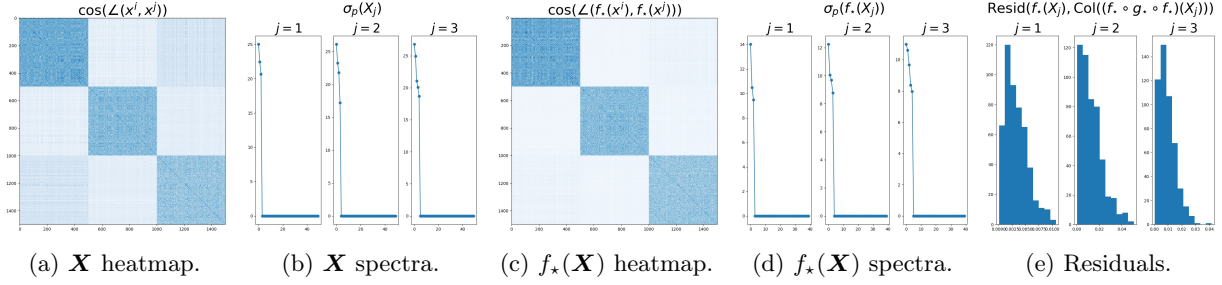


Figure 12: Baseline performance of CTRL-MSP on benign subspaces.

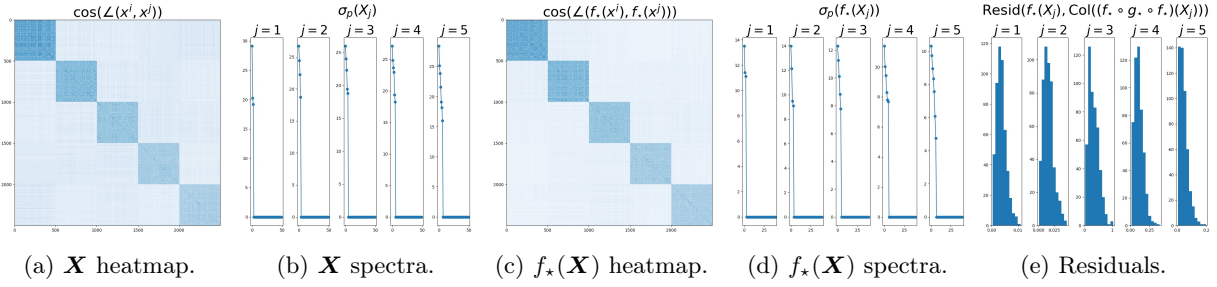


Figure 13: Baseline performance of CTRL-MSP on benign subspaces, with $k = 5$ and $d_S = [3, 4, 5, 6, 7]$. Importantly, the learned representation quality looks very similar to the baseline.

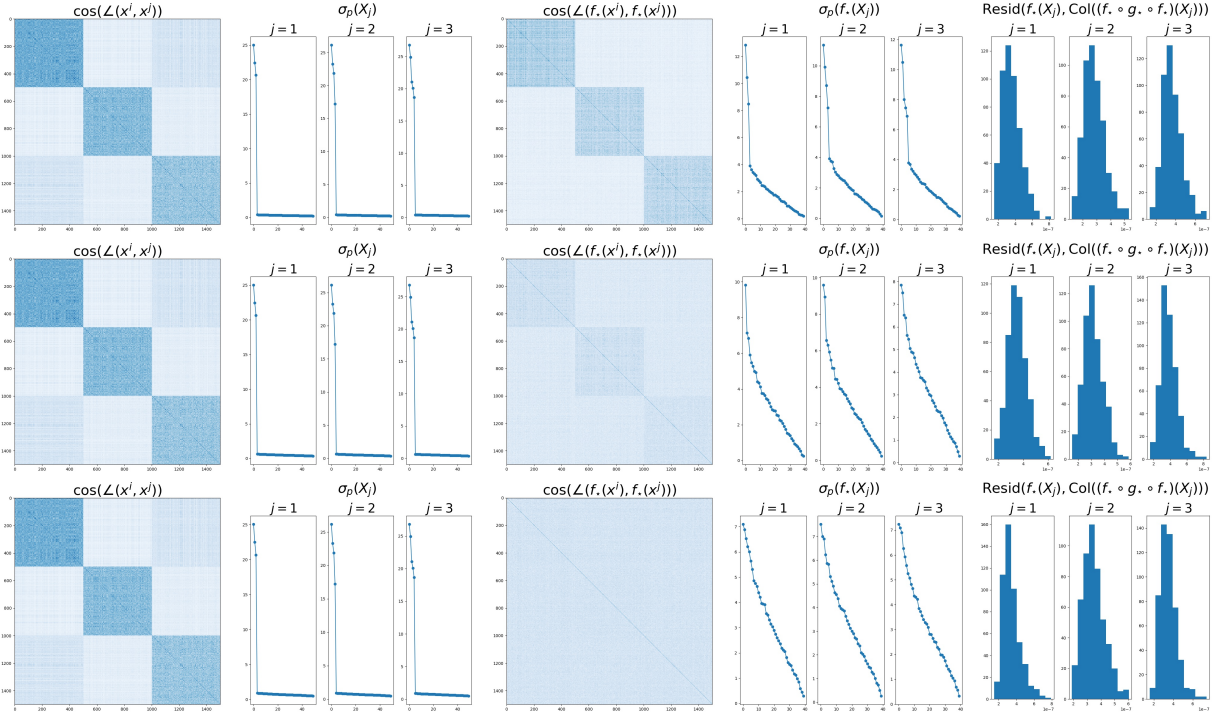


Figure 14: Performance of CTRL-MSP on benign subspaces with varying noise levels σ^2 and $\epsilon = 1.0$. **First row:** performance metrics for $\sigma^2 = 0.01$. **Second row:** the same for $\sigma^2 = 0.025$. **Third row:** the same for $\sigma^2 = 0.05$. We observe a phase transition effect; for $\sigma^2 = 0.01$ the representations look nearly as good as in the noise-free case, while with higher noise the representations degenerate completely.

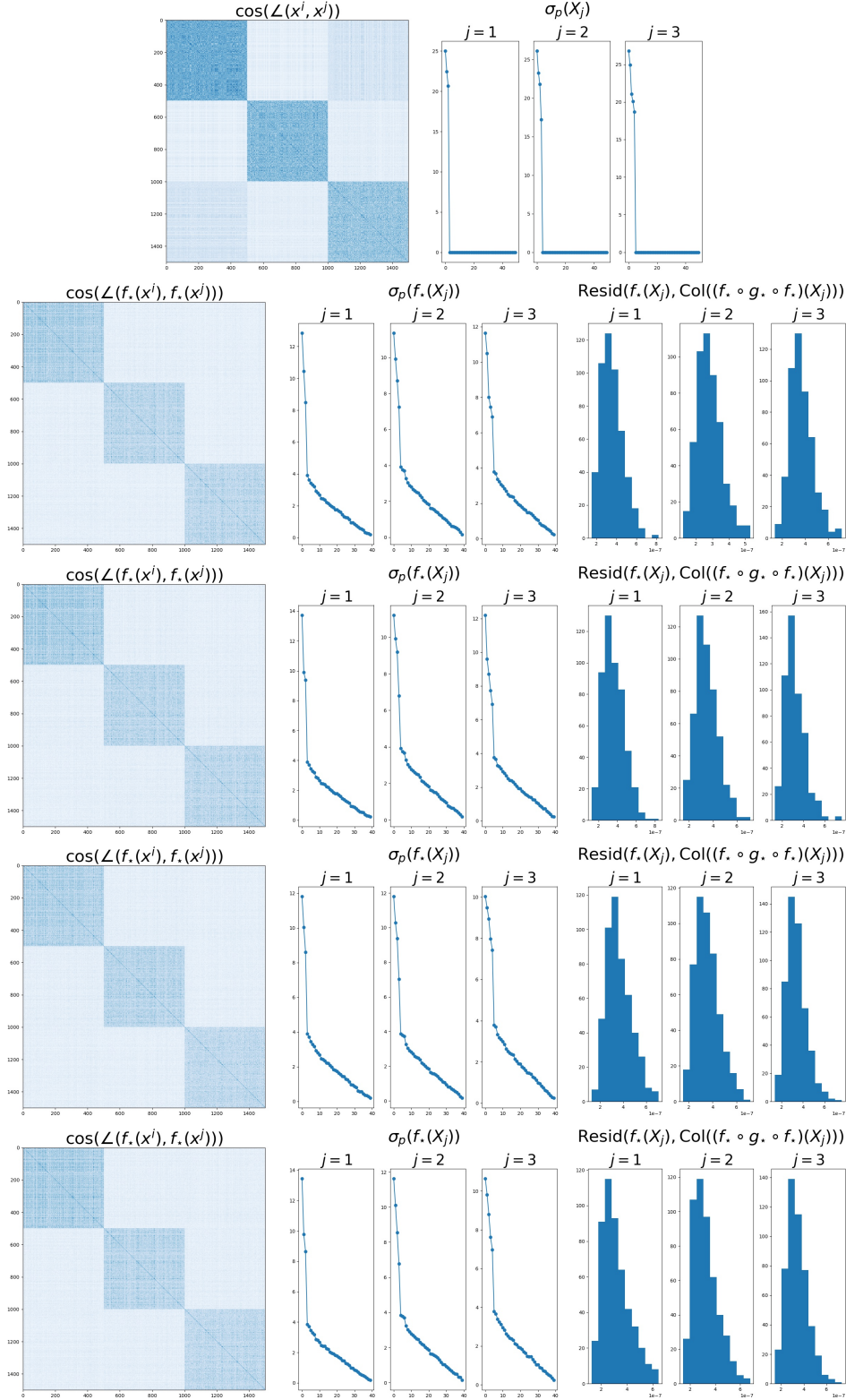


Figure 15: Performance of CTRL-MSP on benign subspaces, varying the parameter ε^2 using noise level $\sigma^2 = 0.01$. **First row:** heatmap of pairwise absolute correlations of \mathbf{X} and spectra of each \mathbf{X}_j . **Second row:** performance metrics for $\varepsilon^2 = 1.0$. **Third row:** the same for $\varepsilon^2 = 0.75$. **Fourth row:** the same for $\varepsilon^2 = 0.5$. **Fifth row:** the same for $\varepsilon^2 = 0.25$. One notes that the performance of the algorithm is *robust* to the choice of ε^2 , meaning that this hyperparameter selection is empirically not very significant, so long as it is small enough.

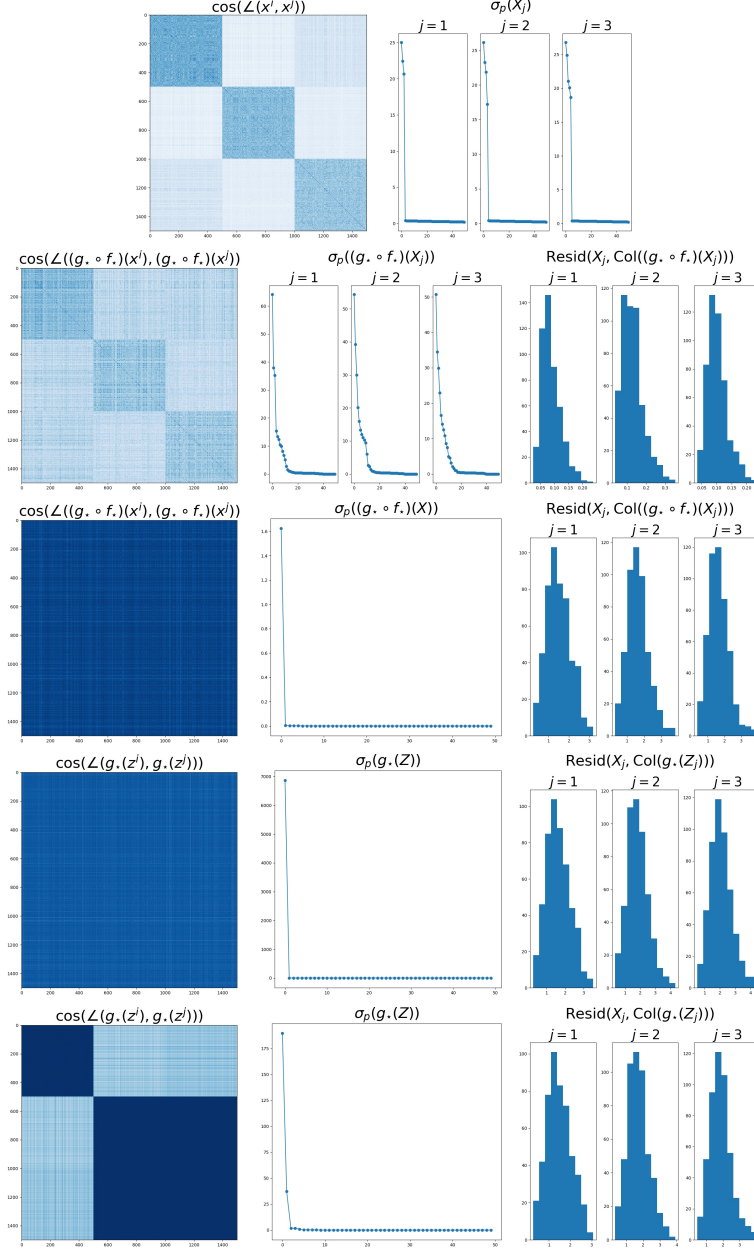


Figure 16: Comparison of CTRL-MSP with CVAE, CGAN, and InfoGAN for benign data using noise level $\sigma^2 = 0.01$. **First row:** heatmap of \mathbf{X} and spectra of each \mathbf{X}_j . **Second row:** heatmap of $g_*(f_*(\mathbf{X}))$, spectra of each $g_*(f_*(\mathbf{X}_j))$, and projection residuals between each \mathbf{X}_j and $\text{Col}(g_*(f_*(\mathbf{X}_j)))$, where f_* and g_* are trained via CTRL-MSP. **Third row:** the same quantities are plotted, where this time g_* is trained via a CVAE. **Fourth row:** heatmap of $g_*(\mathbf{Z})$, spectra of each $g_*(\mathbf{Z}_j)$, and projection residuals between each \mathbf{X}_j and $\text{Col}(g_*(\mathbf{Z}_j))$, where g_* is trained via a CGAN using noise dimension 40 (i.e., such that the columns of \mathbf{Z} are distributed according to $\mathcal{N}(\mathbf{0}_{40}, \mathbf{I}_{40})$). **Fifth row:** the same quantities are plotted with InfoGAN. Of particular interest: CTRL-MSP is the *only* presented algorithm to learn multiple-dimensional linear structure. Indeed, the reconstructed or generated data for other algorithms all lies on one-dimensional subspaces, as evidenced by the generated or reconstructed data having *exactly one* significantly nonzero singular value.

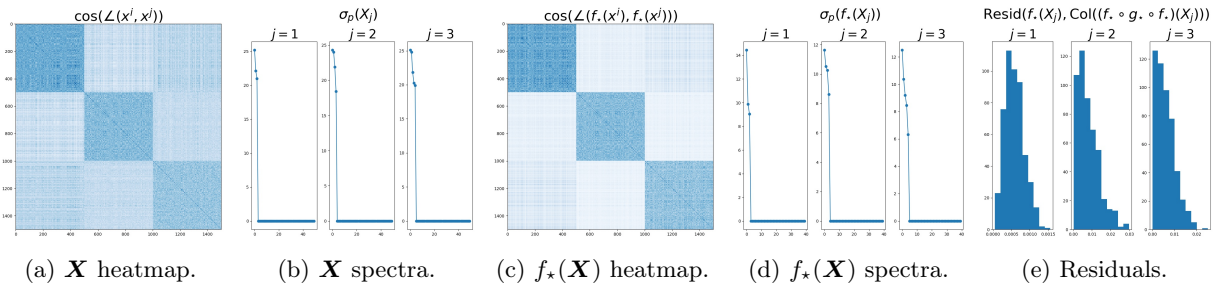


Figure 17: The same as Figure 12, but with coherent subspaces.

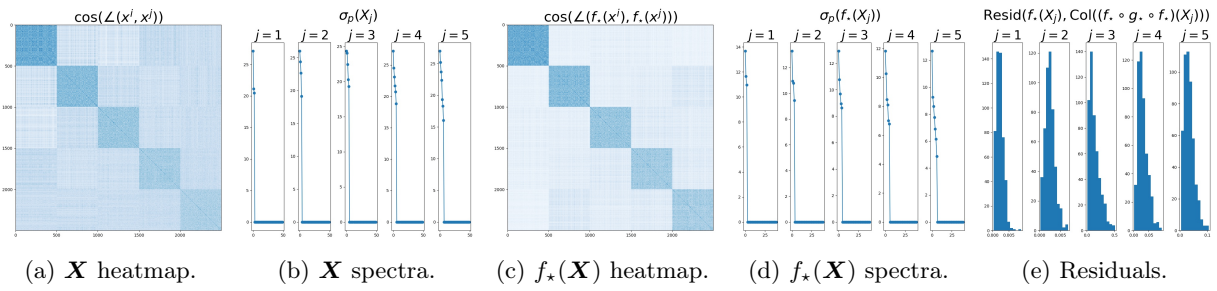


Figure 18: The same as Figure 13, but with coherent subspaces.

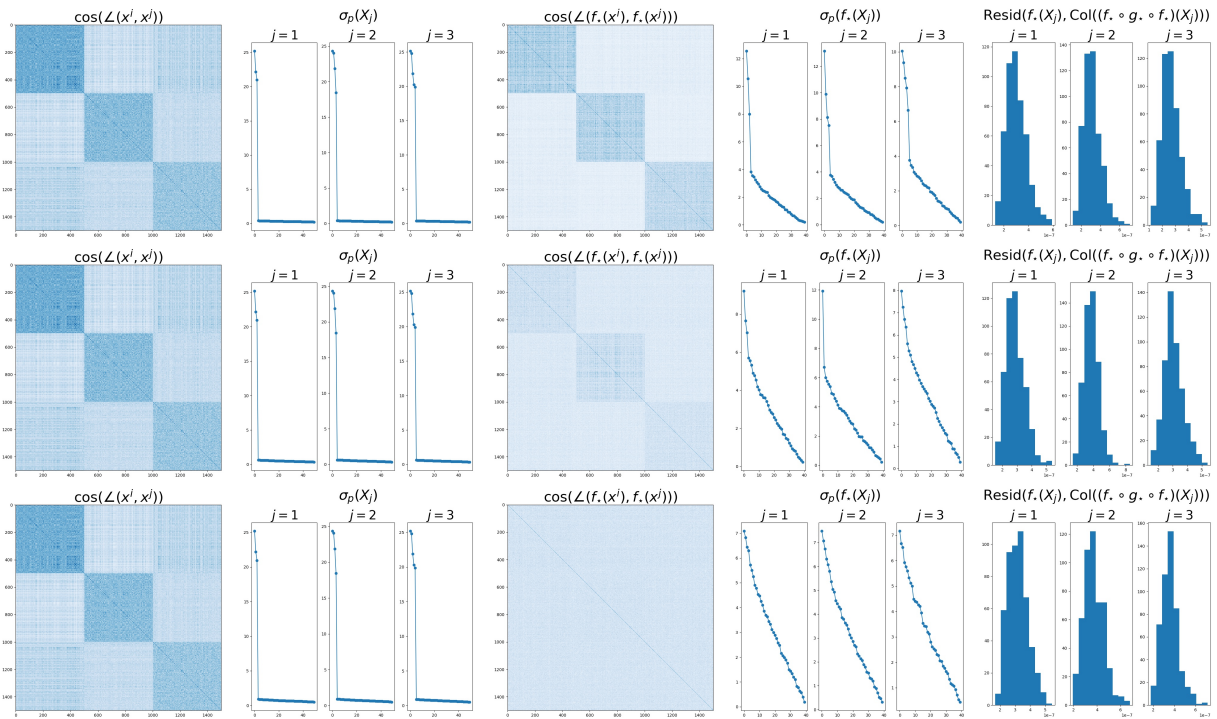


Figure 19: The same as Figure 14, but with coherent subspaces.

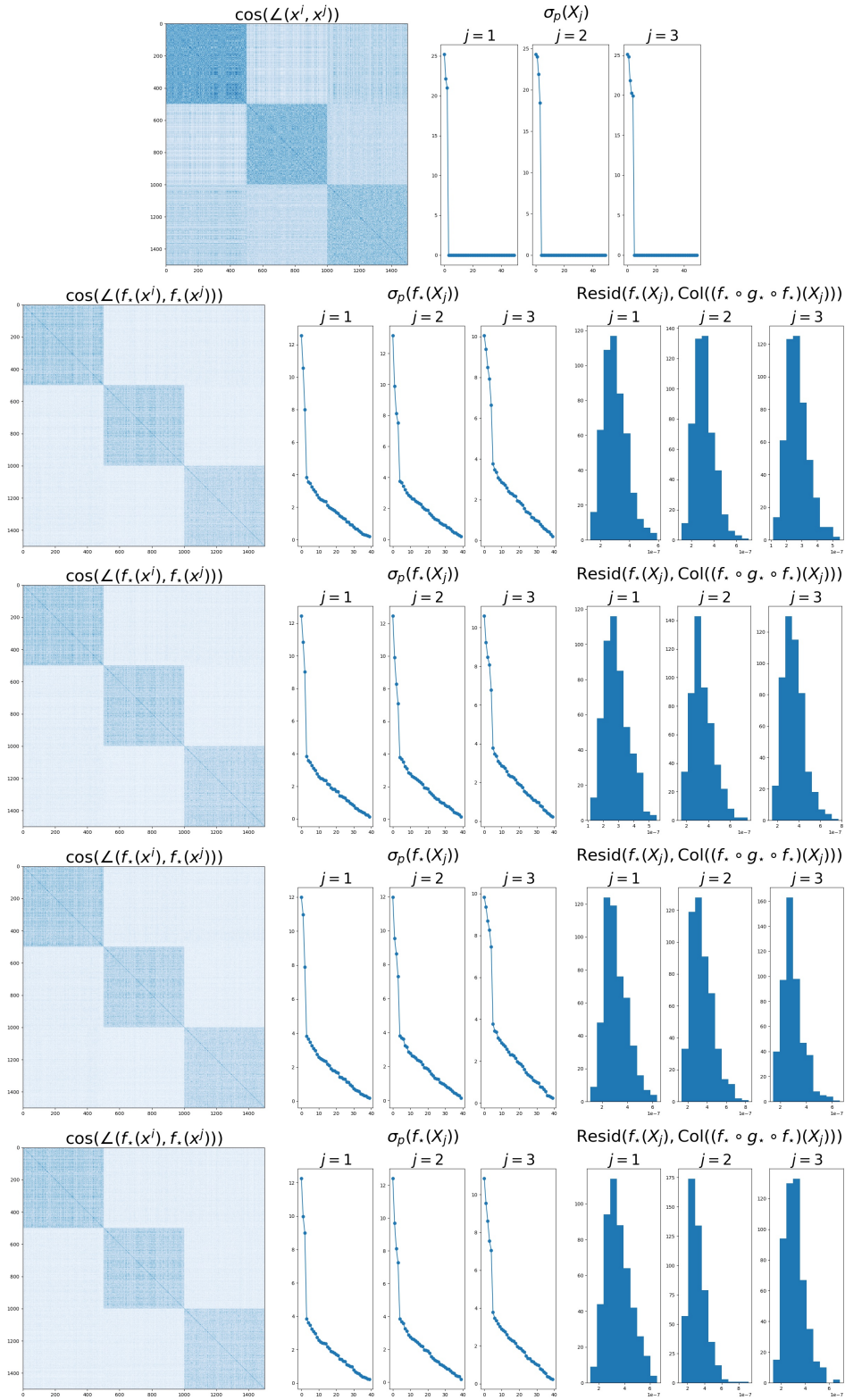


Figure 20: The same as Figure 15, but with coherent subspaces.

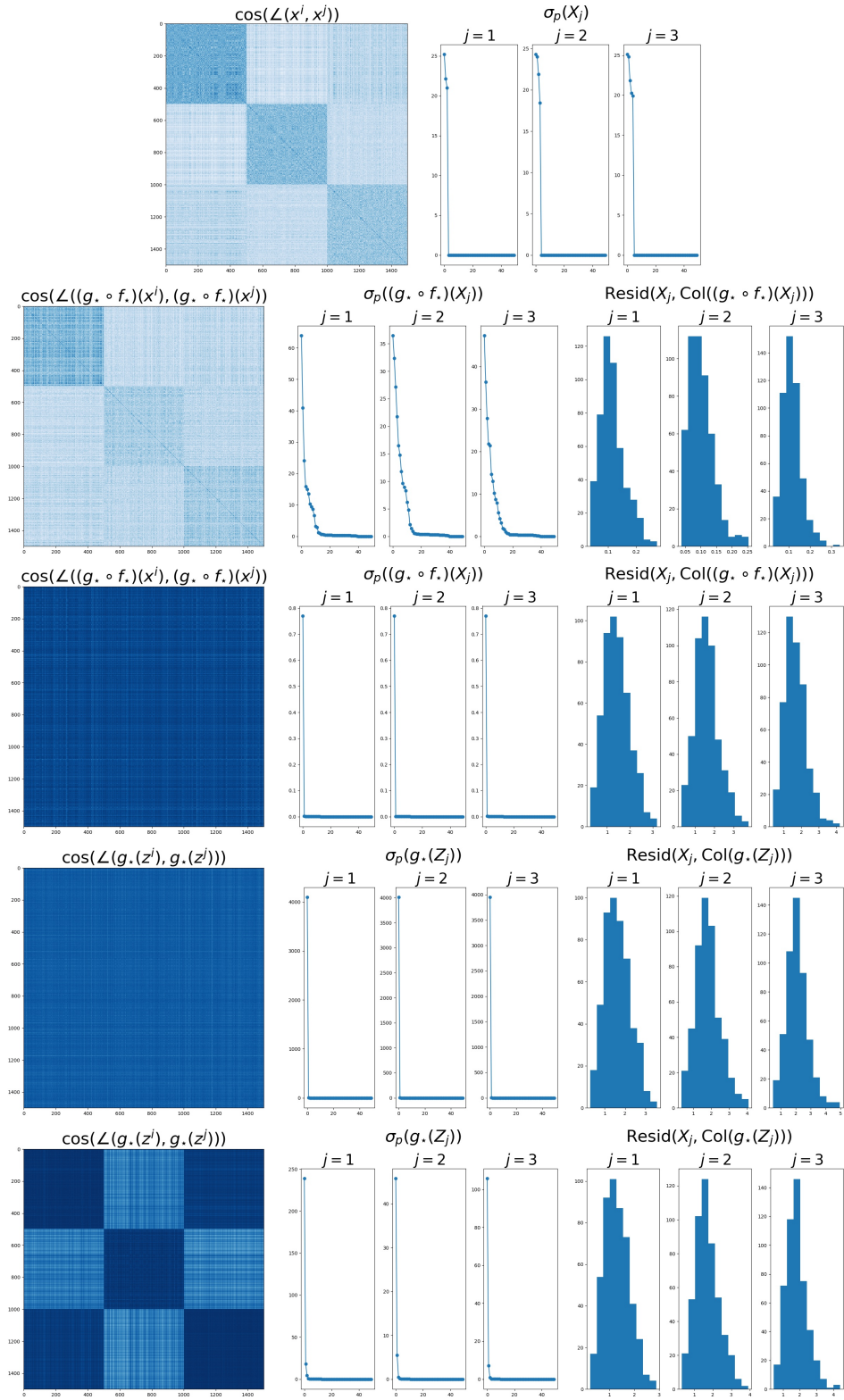


Figure 21: The same as Figure 16, but with coherent subspaces.